SOUND WAVE SCATTERING FROM AN ELASTIC SPHERICAL SHELL

C.J. PARTRIDGE

MRL-TR-91-10

JANUARY 1993

MATERIALS RESEARCH LABORATORY
DSTO

Sound Wave Scattering from an Elastic Spherical Shell

C.J. Partridge

MRL Technical Report
MRL-TR-91-10

Abstract

The Helmholtz integral equation may be formulated by combining the scalar wave equation and Euler's equation for motion within a fluid. The solution to this integral equation yields the radiated pressure from a submerged vibrating body. The solution obtained from applying Hamilton's variational principle governs the response to a given surface pressure excitation. These two solutions may be used in conjunction to investigate the scattering of incident sound waves from shell-like bodies. In this report, the scattering from a submerged steel spherical shell having a thickness to radius ratio of 0.01 is investigated for ka values up to 8.

MATERIALS RESEARCH LABORATORY

Published by

DSTO Materials Research Laboratory
Cordite Avenue, Maribyrnong
Victoria, 3032 Australia

Telephone: (03) 246 8111
Fax: (03) 246 8999

AR No. 006-356

APPROVED FOR PUBLIC RELEASE

Author

C.J. Partridge

Chris Partridge graduated with a BSc from RMIT and was awarded an MSc from the University of Melbourne in 1989. Later that year he joined MRL where he has carried out theoretical investigations on the acoustic scattering from underwater bodies. He is currently undertaking a PhD in the mathematics department at La Trobe University.

Contents

Sound Wave Scattering from an Elastic Spherical Shell

1. Introduction

Anechoic coatings have the ability to modify the scattering behaviour of sound waves incident upon a body. The first step in the investigation of anechoic coatings is to consider their effects when applied to simple objects such as a sphere or a spherical shell. Before an analysis of this is possible, it is necessary to have a firm grasp of the scattering characteristics of the body prior to the application of the coating.

The purpose of this report is to extend the analysis given in Partridge [1] for the rigid sphere, to the scattering behaviour of a thin elastic spherical shell. The mathematical derivation of the scattered pressure requires the use of both the Helmholtz integral equation and Hamilton's variational principle. This analysis essentially follows that given in the work of Junger and Feit [2]. Combining this with various scattering parameters in the literature [3-7], such as target strength, back-scattering cross-section, reflection factor and intensity field around the body, the overall behaviour of the elastic shell, may be analysed. In a subsequent report, these results will be compared with those obtained from coated spherical shells.

1.1 Helmholtz Integral Equation

A sound wave can be thought of as a time dependent pressure fluctuation P around the static pressure P_s in a compressible fluid such as water. The temporal and spatial variations of this fluctuation are governed by the wave equation

$$\nabla^2 P = \frac{1}{c^2} \frac{\partial P^2}{\partial t^2} \tag{1.1}$$

where c is the wave propagation speed through the fluid. If we restrict ourselves to steady-state situations, where the pressure varies periodically with time, i.e.

$$P(\underset{\sim}{r}, t) = P(\underset{\sim}{r})e^{-i\omega t} \tag{1.2}$$

then the above reduces to the "Helmholtz" or "steady-state" wave equation

$$(\nabla^2 + k^2)P(\underset{\sim}{r}) = 0 \tag{1.3}$$

where the acoustic wavenumber is given by $k = \omega/c$. Euler's equation of motion within a non-viscous, homogeneous fluid is given by

$$\nabla P = -\rho \frac{\partial \mathbf{v}}{\partial t} \tag{1.4}$$

where ρ and $\mathbf{v}$ are the density and velocity respectively. For a non-viscous fluid, pressure can act only in a direction normal to the surface boundary S_o, and letting the normal component of velocity to the boundary be given by

$$\dot{w}(\underset{\sim}{r}_o, t) = \dot{w}(\underset{\sim}{r}_o)e^{-i\omega t} \tag{1.5}$$

where r_o defines the surface S_o, the above boundary condition reduces to

$$\frac{\partial P}{\partial n} = (i\omega\rho)\dot{w} \quad \text{on } S_o \tag{1.6}$$

where n is the unit outward normal to S_o. The pressure radiated from a body vibrating with a surface velocity distribution w, is governed by equations (1.3) and (1.6). From Partridge [1], these two equations may be combined to form the Helmholtz Integral equation

$$P(\underset{\sim}{r}) = -\int\int\left[P(\underset{\sim}{r}_o)\frac{\partial G}{\partial n} - (i\omega\rho)G(\underset{\sim}{r}|\underset{\sim}{r}_o)\dot{w}(\underset{\sim}{r}_o)\right]dS(\underset{\sim}{r}_o) \quad \underset{\sim}{r} \text{ outside } S_o \tag{1.7}$$

where Green's function $G(r \mid r_o)$ represents the field at a point r due to a unit impulse located at r_o. If the Green's function satisfies the Neumann boundary condition

$$\frac{\partial G}{\partial n} = 0 \quad \text{on the boundary } S_o \tag{1.8}$$

then the Helmholtz integral equation reduces to the simple integral

$$P(\underset{\sim}{r}) = (i\omega\rho) \iint \left[G(\underset{\sim}{r}|\underset{\sim}{r}_o) \dot{w}(\underset{\sim}{r}_o) \right] dS_o \tag{1.9}$$

1.2 *Pressure Field for a Spherical Radiator*

For a vibrating spherical body of radius a, the above integral becomes

$$P(r,\vartheta) = (i\omega\rho)(2\pi a^2) \int_o^{\pi} \left[G(\underset{\sim}{r},\vartheta|a,\vartheta_o) \dot{w}(\vartheta_o) \right] \sin\vartheta_o \, d\vartheta_o \tag{1.10}$$

The Green's function and surface velocity are given [1] by

$$G(r,\vartheta|a,\vartheta_o) = \frac{1}{4\pi ka^2} \sum_{n=o}^{\infty} (2n+1) P_n(\cos\vartheta) P_n(\cos\vartheta_o) \frac{h_n(kr)}{h_n'(ka)} \tag{1.11}$$

$$\dot{w}(\vartheta) = \sum_{n=o}^{\infty} \dot{W}_n P_n(\cos\vartheta) \tag{1.12}$$

where $P_n(\cos\varphi)$ and $h_n(kr)$ are the Legendre and Hankel functions respectively and

$$\dot{W}_n = \frac{(2n+1)}{2} \int_{-1}^{1} P_n(\eta) \dot{w}(\eta) \, d\eta, \quad \eta = \cos\vartheta \tag{1.13}$$

Substituting equations (1.11) and (1.12) into (1.10), yields the pressure radiated from a spherical body

$$P(r,\vartheta) = i(\rho c) \sum_{n=o}^{\infty} \dot{W}_n P_n(\cos\vartheta) \frac{h_n(kr)}{h_n'(ka)} \tag{1.14}$$

This solution will be applied later to obtain the scattered pressure from a spherical shell impacted by plane waves.

1.3 *Radiation Loading*

When a submerged body vibrates, it sets up pressure fluctuations in the surrounding fluid. These fluctuations (termed the radiation loading) then act back on the structure. This radiation loading modifies the forces acting on the

structure, and since these pressures depend on the velocity at which the structure vibrates, a feedback coupling between the fluid and the structure exists. The ratio of surface pressure to the surface velocity is defined as the specific acoustic impedance. In modal form this becomes

$$z_n = f_n / \dot{W}_n \tag{1.15}$$

where

$$P(a,\vartheta) = \sum_{n=0}^{\infty} f_n P_n(\cos\vartheta), \quad \dot{w}(\vartheta) = \sum_{n=0}^{\infty} \dot{W}_n P_n(\cos\vartheta) \tag{1.16}$$

The specific acoustic impedance measured on the surface of the source, determines the radiation loading, and may be expanded into its real and imaginary components which are designated by r_n and ωm_n. Therefore, equation (1.15) may be rewritten as

$$\begin{aligned} f_n &= (r_n - i\omega m_n)\dot{W}_n \\ &= r_n \dot{W}_n + m_n \ddot{W}_n \end{aligned} \tag{1.17}$$

The surface pressure is the sum of two terms, (1) a term proportional to the surface particle velocity w embodying a resistive or damping force, which represents the energy lost by the pulsating sphere in the form of radiated acoustic energy, and (2) a term proportional to the surface particle acceleration associated with the mass of fluid set into motion by the pulsating surface of the spherical source. Using equation (1.14) for the radiated pressure, the modal acoustic impedance for a spherical body becomes

$$\begin{aligned} z_n &= i(\rho c)\frac{h_n(ka)}{h_n'(ka)} \\ &= r_n - i\omega m_n \end{aligned} \tag{1.18}$$

where

$$\begin{aligned} r_n &= (\rho c) Re\left[\frac{i h_n(ka)}{h_n'(ka)}\right] \\ &= (\rho c)[(ka)|h_n'(ka)|]^{-2} \\ &= \frac{(\rho c)(ka)^{2n+2}}{(n+1)^2[1.3\ldots(2n-1)]^2}, \quad (ka)^2 << |2n-1| \\ &= (\rho c), \quad (ka) >> n^2+1 \end{aligned} \tag{1.19}$$

and

$$
\begin{aligned}
m_n &= -\frac{\rho c}{\omega} Im\left[\frac{ih_n(ka)}{h_n'(ka)}\right] \\
&= -\frac{\rho a}{ka}\frac{j_n'(ka)j_n(ka)+y_n'(ka)y_n(ka)}{|h_n'(ka)|^2} \qquad (1.20)\\
&= \rho a(n+1)^{-1}, \qquad (ka)^2 << |2n-1| \\
&= \rho a(ka)^{-2}, \qquad (ka) >> n^2+1
\end{aligned}
$$

2. *Equations of Motion for a Spherical Shell*

2.1 *Formulation of Problem*

The solution to the equations of motion for an air-filled spherical shell subjected to an excitation pressure, yields the velocity distribution around the shell's surface. The surface pressure excites the normal vibration modes of the shell. The exterior boundary pressure and the displacements on a spherical surface (called the shell middle surface) which is located centrally between the physical surface boundaries of the shell, may be expressed as

$$
\begin{aligned}
P_a(a,\vartheta) &= \sum_{n=o}^{\infty} f_n P_n(\eta), \quad \eta = \cos\vartheta \\
u(\vartheta) &= \sum_{n=o}^{\infty} U_n(1-\eta^2)^{1/2}\, dP_n(\eta)/d\eta, \quad w(\vartheta) = \sum_{n=o}^{\infty} W_n P_n(\eta)
\end{aligned} \qquad (2.1)
$$

where u and w are the "tangential" and "normal" displacement components respectively. The velocity distribution is related to the displacements via $u = (-i\omega)u$ and $w = (-i\omega)w$. In order to derive the equations of motion, several assumptions must be made:

(a) Displacements are assumed small compared with the shell thickness.

(b) The shell thickness is small compared with the radius of curvature of the sphere.

(c) Fibres of the shell initially perpendicular to the shell middle surface remain so after deformation and are themselves not subject to elongation.

(d) The normal stress σ_{rr} acting on planes parallel to the shell middle surface is negligible in comparison with other stresses.

These assumptions allow us to reduce the problem of shell deformation, to the study of middle surface deflection. The equations of motion are derived from

displacements. Hamilton's principle states that if the work done on the shell by the external pressure causes the displacements to undergo a variation between the times t_0 and t_1, then

$$\delta \int_{t_0}^{t_1} (E_k + E_s) dt + \int_{t_0}^{t_1} \delta w \, dt = 0 \tag{2.2}$$

where E_k, E_s are the kinetic and strain energies, and δw is the work done by the pressure. Consider a thin spherical shell of thickness h and mean radius "a" as shown in Figure 1. In this derivation, only non-torsional axisymmetric motions of the shell are considered, making the variables independent of the angular coordinate ϕ. The shell displacements U_s and W_s can be written in terms of the middle-surface displacements u, and w using [2]

$$U_s = \left(1 + \frac{x}{a}\right) u - \left(\frac{x}{a}\right) \frac{\partial w}{\partial \vartheta}, \qquad W_s = w \tag{2.3}$$

where $x = r - a$. The total kinetic energy of the system may be written as

$$\begin{aligned} E_k &= \frac{1}{2} \rho_s \iiint (\dot{U}_s^2 + \dot{W}_s^2) \, dv \\ &= \frac{1}{2} \rho_s \int_0^{2\pi} \int_0^{\pi} \int_{-h/2}^{+h/2} (\dot{U}_s^2 + \dot{W}_s^2) \, a^2 \sin\vartheta \, d\phi \, d\vartheta \, d\lambda \\ &= \pi \rho_s h a^2 \int_0^{\pi} (\dot{u}^2 + \dot{w}^2) \sin\vartheta \, d\vartheta \end{aligned} \tag{2.4}$$

In spherical coordinates, the strains and stresses are

$$\begin{aligned} \varepsilon_{\vartheta\vartheta} &= \frac{1}{(a+x)} \left(\frac{\partial U_s}{\partial \vartheta} + W_s \right) = \frac{1}{a} \left(\frac{\partial u}{\partial \vartheta} + w \right) + \frac{x}{a^2} \left(\frac{\partial u}{\partial \vartheta} - \frac{\partial^2 w}{\partial \vartheta^2} \right) \\ \varepsilon_{\phi\phi} &= \frac{1}{(a+x)} (\cot\vartheta U_s + W_s) = \frac{1}{a} (\cot\vartheta u + w) + \frac{x}{a^2} \cot\vartheta \left(u - \frac{\partial w}{d\vartheta} \right) \end{aligned} \tag{2.5}$$

$$\sigma_{\vartheta\vartheta} = \frac{E}{(1-\nu^2)} (\varepsilon_{\vartheta\vartheta} + \nu \varepsilon_{\phi\phi}), \quad \sigma_{\phi\phi} = \frac{E}{(1-\nu^2)} (\varepsilon_{\phi\phi} + \nu \varepsilon_{\vartheta\vartheta}) \tag{2.6}$$

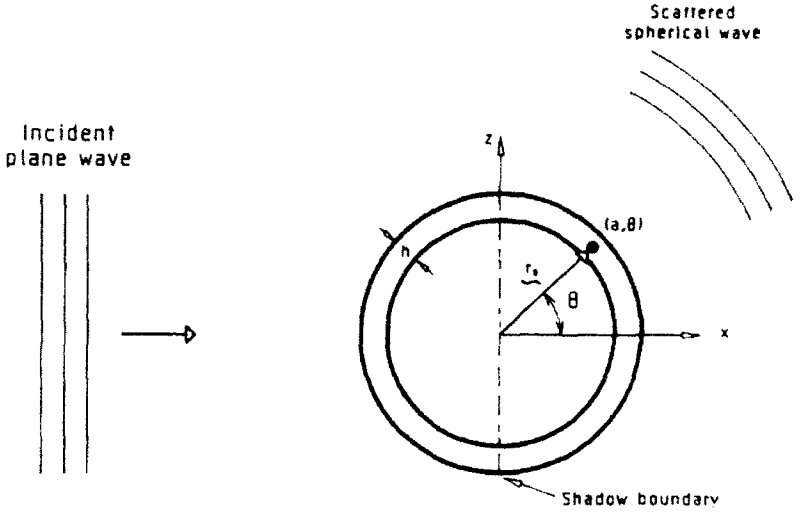

Figure 1: Sound scattering from an elastic spherical shell.

The strain energy of the system in terms of these components is

$$
\begin{aligned}
E_s &= \iiint \left(\frac{1}{2} \sigma_{ij} \varepsilon_{ij} \right) dV \\
&+ \frac{1}{2} \int_0^{2\pi} \int_0^{\pi} \int_{-h/2}^{+h/2} (\sigma_{\vartheta\vartheta} \varepsilon_{\vartheta\vartheta} + \sigma_{\phi\phi} \varepsilon_{\phi\phi}) a^2 \sin\vartheta \, d\vartheta \, d\phi \, dx \\
&= \frac{\pi E h}{(1-\nu^2)} \int_0^{\pi} \left[\left(\frac{\partial u}{\partial \vartheta} + w \right)^2 + (\cot\vartheta u + w)^2 + 2\nu \left(\frac{\partial u}{\partial \vartheta} + w \right) (\cot\vartheta u + w) \right] \sin\vartheta \, d\vartheta \\
&+ \frac{\pi E h \beta^2}{(1-\nu^2)} \int_0^{\pi} \left[\left(\frac{\partial u}{\partial \vartheta} - \frac{\partial^2 w}{\partial \vartheta^2} \right)^2 + \cot^2\vartheta \left(u - \frac{\partial w}{\partial \vartheta} \right)^2 \right. \\
&\left. + 2\nu \cot\vartheta \left(\frac{\partial u}{\partial \vartheta} - \frac{\partial^2 w}{\partial \vartheta^2} \right) \left(u - \frac{\partial w}{\partial \vartheta} \right) \right] \sin\vartheta \, d\vartheta
\end{aligned}
\tag{2.7}
$$

where the contribution of the bending stresses to the strain energy is represented by the term $\beta^2 = h^2/12a^2$. The work done by the surface pressure (applied normal to the undeformed shell surface) is

$$W = \iint P_a\, w\, dS = a^2 \int_0^{2\pi} \int_0^{\pi} P_a\, w \sin\vartheta\, d\vartheta\, d\phi$$
$$= (2\pi a^2) \int_0^{\pi} P_a\, w \sin\vartheta\, d\vartheta \tag{2.8}$$

Applying Hamilton's principle with respect to the variations δu and δv to obtain the equations of motion for the spherical shell yields

$$(1+\beta^2)\left(\frac{\partial^2 u}{\partial\vartheta^2} + \cot\vartheta\,\frac{\partial u}{\partial\vartheta} - (\nu + \cot^2\vartheta)u\right) - \beta^2\,\frac{\partial^3 w}{\partial\vartheta^3}$$
$$-\beta^2\cot\vartheta\,\frac{\partial^2 w}{\partial\vartheta^2} + \left((1+\nu) + \beta^2(\nu + \cot^2\vartheta)\right)\frac{\partial w}{\partial\vartheta} - \frac{a^2\ddot{u}}{c_p^2} = 0$$
$$\beta^2\,\frac{\partial^3 u}{\partial\vartheta^3} + 2\beta^2\cot\vartheta\,\frac{\partial^2 u}{\partial\vartheta^2} - \left((1+\nu)(1+\beta^2) + \beta^2\cot^2\vartheta\right)\frac{\partial u}{\partial\vartheta}$$
$$+\cot\vartheta\left((2-\nu+\cot^2\vartheta)\beta^2 - (1+\nu)\right)u - \beta^2\,\frac{\partial^4 w}{\partial\vartheta^4} - 2\beta^2\cot\vartheta\,\frac{\partial^3 w}{\partial\vartheta^3}$$
$$+\beta^2\left(1+\nu+\cot^2\vartheta\right)\frac{\partial^2 w}{\partial\vartheta^2} - \beta^2\cot\vartheta\left(2-\nu+\cot^2\vartheta\right)\frac{\partial w}{\partial\vartheta} - 2(1+\nu)w - \frac{a^2\ddot{w}}{c_p^2} = \frac{-P_a(1-\nu^2)a^2}{Eh} \tag{2.9}$$

where the wave speed in the shell material c_p is given by

$$c_p^2 = \frac{E}{\rho_s(1-\nu^2)} \tag{2.10}$$

Introducing the variable $\eta = \cos\varphi$ and assuming harmonic time variation, the foregoing set of equations may be rewritten in the form

$$L_{uu}(u) + L_{uw}(w) + \Omega^2 u = 0$$
$$L_{wu}(u) + L_{ww}(w) + \Omega^2 w = -P_a\left(\frac{a^2(1-\nu^2)}{Eh}\right) \tag{2.11}$$

where

$$
\begin{aligned}
L_{uu} &= (1+\beta^2)\left((1-\eta^2)^{1/2}\frac{d^2}{d\eta^2}(1-\eta^2)^{1/2}+(1-\nu)\right)\\
L_{uw} &= (1-\eta^2)^{1/2}\left([\beta^2(1-\nu)-(1+\nu)]\frac{d}{d\eta}+\beta^2\frac{d}{d\eta}\nabla_\eta^2\right)\\
L_{wu} &= -\left([\beta^2(1-\nu)-(1+\nu)]\frac{d}{d\eta}(1-\eta^2)^{1/2}+\beta^2\nabla_\eta^2\frac{d}{d\eta}(1-\eta^2)^{1/2}\right)\\
L_{ww} &= -\beta^2\nabla_\eta^4-\beta^2(1-\nu)\nabla_\eta^2-2(1+\nu)
\end{aligned}
\tag{2.12}
$$

and

$$
\nabla_\eta^2 = \frac{d}{d\eta}(1-\eta^2)\frac{d}{d\eta} \tag{2.13}
$$

Substituting u and w for their respective series representation, yields

$$
\begin{aligned}
&[\Omega^2-(1+\beta^2)(\nu+\lambda_n-1)]U_n-[\beta^2(\nu+\lambda_n-1)+(1+\nu)]W_n = 0\\
&-\lambda_n[\beta^2(\nu+\lambda_n-1)+(1+\nu)]U_n+[\Omega^2-2(1+\nu)-\beta^2(\nu+\lambda_n-1)]W_n = -\left[\frac{a^2(1-\nu^2)}{Eh}\right]f_n
\end{aligned}
\tag{2.14}
$$

where $\lambda_n = n(n+1)$. Therefore to obtain the response of the shell, the above linear equations are solved for each n, to obtain U_n and W_n and then substituted into equations (2.1) for u and w to yield the middle surface displacements of the shell due to the excitation pressure P_s.

2.2 *Natural Frequencies of the Shell*

2.2.1 *In a Vacuum*

The resonant frequencies for the free vibration of a spherical shell may be obtained by setting f_n to zero in equation (2.14), and then eliminating U_n and W_n. This yields the frequency equation

$$
\begin{aligned}
\Omega^4 &- \left((1+3\nu+\lambda_n)-\beta^2(1-\nu-\lambda_n^2-\nu\lambda_n)\right)\Omega^2+(\lambda_n-2)(1-\nu^2)\\
&+\beta^2\left(\lambda_n^3-4\lambda_n^2+\lambda_n(5-\nu^2)-2(1-\nu^2)\right) = 0
\end{aligned}
\tag{2.15}
$$

where the non-dimensional frequency Ω is defined as $(ka)(c/c_p)$ and c_p is given by equation (2.10). The above equation may be written in the form

$$\left[\Omega^2 - (\Omega_n^{(1)})^2\right]\left[\Omega^2 - (\Omega_n^{(2)})^2\right] = 0 \tag{2.16}$$

where $\Omega_n^{(1)}$, $\Omega_n^{(2)}$ are the two resonant frequencies, of which $\Omega_n^{(2)}$ is the larger. For each mode characterized by a specific value of $n > 0$, there are two distinct positive real resonant frequencies, but for $n = 0$ corresponding to what is called the breathing mode, there is only one real positive frequency, the other being imaginary.

2.2.2 *Submerged in Water*

In order to determine the resonant frequencies of the submerged shell, we need to go back to the equations (2.14), i.e.

$$[\Omega^2 - (1+\beta^2)(\nu+\lambda_n-1)]U_n - [\beta^2(\nu+\lambda_n-1)+(1+\nu)]W_n = 0$$

$$-\lambda_n[\beta^2(\nu+\lambda_n-1)+(1+\nu)]U_n + [\Omega^2-2(1+\nu)-\beta^2(\nu+\lambda_n-1)]W_n = -\left[\frac{a^2(1-\nu^2)}{Eh}\right]f_n \tag{2.17}$$

To determine these frequencies, a radiation damping term must be introduced. The loading, in the absence of a driving force, is expressed in terms of the specific acoustic impedance as

$$\begin{aligned} P_s &= -\sum_{n=o}^{\infty} z_n W_n P_n(\cos\vartheta) \\ &= \sum_{n=o}^{\infty} [(i\omega)r_n + (\omega^2)m_n] W_n P_n(\cos\vartheta) \end{aligned} \tag{2.18}$$

The negative sign arises because the applied pressure was defined previously as positive outward, whilst the radiation loading is positive inward. Therefore, replacing f_n in equation (2.17) with

$$f_n = -[(i\omega)r_n + (\omega^2)m_n]W_n \tag{2.19}$$

yields

$$[\Omega^2 - (1+\beta^2)(\nu+\lambda_n-1)]U_n - [\beta^2(\nu+\lambda_n-1)+(1+\nu)]W_n = 0 \tag{2.20}$$

$$-\lambda_n[\beta^2(\nu+\lambda_n-1)+(1+\nu)]U_n + \left[\Omega^2\left(1+\frac{m_n}{\rho_s h}\right)+i\Omega\left(\frac{ar_n}{c_p\rho_s h}\right)-2(1+\nu)-\beta^2(\nu+\lambda_n-1)\right]W_n = 0$$

Combining equations (2.20), and noting that the natural frequencies are the roots of the real component of the resultant equation yields

$$a_0\Omega^4 + a_1\Omega^2 + a_2 = 0 \tag{2.21}$$

where

$$a_0 = (1 + \frac{m_n}{\rho_s h})$$

$$a_1 = -[2(1+\nu) + \beta^2\lambda_n(\nu+\lambda_n-1) + (1+\beta^2)(\nu+\lambda_n-1)(1+\frac{m_n}{\rho_s h})]$$

$$a_2 = [2(1+\nu) + \beta^2(\nu+\lambda_n-1)](1+\beta^2)(\nu+\lambda_n-1) - \lambda_n[\beta^2(\nu+\lambda_n-1) + (1+\nu)]^2$$

The solution to this equation yields the natural frequencies for a submerged shell. It is a transcendental equation since m_n given by equation (1.20) is frequency dependent.

Listed below are the values that will be used in this report for both the propagation medium and the spherical shell.

Propagation medium

Sound velocity in water	c	=	1500	(m/s)
Water density	ρ	=	1000	(kg/m^3)

Spherical shell (steel)

Mean radius	a	=	1.0	(m)
Shell thickness	h	=	0.01	(m)
Density	ρ_s	=	7700	(kg/m^3)
Young's modulus	E	=	19.5×10^{10}	(Pa)
Poisson's ratio	ν	=	0.29	(-)

The natural frequencies for the above steel shell in a vacuum and submerged in water, are tabulated in Table 1. From the table, it may be seen that radiation loading reduces the natural frequencies of the shell.

Table 1: Effect of submergence on the normal modes of a spherical shell

		Dimensionless Natural Frequency Ω		Dimensionless Frequency parameter ka	
Branch	n	In vacuo	Submerged	In vacuo	Submerged
Lower					
$\Omega_n^{(1)}$	0	imaginary	imaginary	0.00	0.00
	1	0.000	0.000	0.00	0.00
	2	0.705	0.325	2.47	1.14
	3	0.834	0.411	2.92	1.44
	4	0.886	0.468	3.10	1.64
	5	0.912	0.514	3.19	1.80
	6	0.930	0.548	3.25	1.92
	7	0.944	0.582	3.31	2.04
	8	0.958	0.610	3.36	2.14
	9	0.975	0.639	3.41	2.24
Upper					
$\Omega_n^{(2)}$	0	1.606	1.156		
	1	1.967	1.763		
	2	2.715	2.367		
	3	3.360	3.417		
	4	4.592	4.444		
	5	5.572	5.460		
	6	6.559	6.471		
	7	7.550	7.478		
	8	8.544	8.483		
	9	9.539	9.487		

2.3 *Velocity Response of Shell due to an Arbitrary Surface Excitation*

2.3.1 *In a Vacuum*

The middle-surface displacements caused by a surface excitation

$$P_a(\vartheta) = \sum_{n=0}^{\infty} f_n P_n(\cos\vartheta) \tag{2.22}$$

were earlier expressed as

$$u(\vartheta) = \sum_{n=0}^{\infty} U_n (1-\eta^2)^{1/2} \, dP_n(\eta)/d\eta, \quad w(\vartheta) = \sum_{n=0}^{\infty} W_n P_n(\eta) \tag{2.23}$$

where the coefficients of U_n and W_n are given by

$$[\Omega^2 - (1+\beta^2)(\nu-\lambda_n-1)]\,U_n - [\beta^2(\nu+\lambda_n-1)+(1+\nu)]\,W_n = 0$$

$$-\lambda_n[\beta^2(\nu+\lambda_n-1)+(1+\nu)]\,U_n + [\Omega^2-2(1+\nu)-\beta^2\lambda_n(\nu+\lambda_n-1)]\,W_n = -\left[\frac{a^2(1-\nu^2)}{Eh}\right]f_n \tag{2.24}$$

Solving the above for U_n and W_n, yields

$$U_n = -\left[\frac{a^2(1-\nu^2)}{Eh}\right]f_n \frac{[\beta^2(\nu+\lambda_n-1)+(1+\nu)]}{(\Omega^2-\Omega_n^{(1)})^2(\Omega^2-\Omega_n^{(2)})^2}$$

$$W_n = -\left[\frac{a^2(1-\nu^2)}{Eh}\right]f_n \frac{[\Omega^2-(1+\beta^2)(\nu+\lambda_n-1)]}{(\Omega^2-\Omega_n^{(1)})^2(\Omega^2-\Omega_n^{(2)})^2} \tag{2.25}$$

The above may be simplified somewhat by introducing a term known as the modal mechanical impedance Z_n, which is defined as the ratio of the resultant surface pressure to the normal velocity, i.e.

$$\begin{aligned} Z_n &= f_n/(-i\omega W_n) \\ &= -i\left[\frac{\rho_a c_p h}{\Omega a}\right]\frac{[\Omega^2-(\Omega_n^{(1)})^2][\Omega^2-(\Omega_n^{(2)})^2]}{[\Omega^2-(1+\beta^2)(\nu+\lambda_n-1)]} \end{aligned} \tag{2.26}$$

Then for a given excitation pressure the normal velocity may be expressed as

$$w(\vartheta) = \sum_{n=0}^{\infty} (f_n/Z_n)\,P_n(\cos\vartheta) \tag{2.27}$$

2.3.2 *Submerged in Water*

Let the excitation and resultant pressures be represented by

$$P_a(\vartheta) = \sum_{n=0}^{\infty} f_n^a\,P_n(\cos\vartheta), \quad P(\vartheta) = \sum_{n=0}^{\infty} f_n\,P_n(\cos\vartheta) \tag{2.28}$$

Then the resultant pressure may be written in modal form as

$$f_n = f_n^a - z_n W_n \tag{2.29}$$

The resultant pressure is however also related to the modal mechanical impedance via $Z_n = f_n / W_n$. Combining these two expressions yields the resulting normal velocity, i.e.

$$\dot{w}(\vartheta) = \sum_{n=0}^{\infty} \frac{f_n^a}{z_n + Z_n} P_n(\cos\vartheta) \tag{2.30}$$

where z_n and Z_n are given by equations (1.18) and (2.26).

3. *Scattering of a Plane Wave from a Spherical Shell*

Consider a distant point sound source which generates a continuous sound wave. Far away from this source, and over suitably restricted regions, these waves may be said to approximate plane waves. Consider these plane waves to be incident upon a stationary thin elastic spherical shell, whose surface S_o is given by the position vector r_o, shown in Figure 1. The following analysis differs from that of a rigid sphere, in that the scatterer is allowed to deflect elastically. In this situation, the structure's dynamic response radiates a pressure field which further modifies the sound field.

If we define a wavenumber vector k, whose magnitude is k and which lies in the direction of wave propagation, then the incident pressure wave may be written as

$$P_i(\underset{\sim}{r},t) = P_o \exp i(\underset{\sim}{k}\cdot\underset{\sim}{r} - \omega t) \tag{3.1}$$

In spherical coordinates, a wave incident from the $\vartheta = 180°$ direction is represented by

$$P_i(r,\vartheta) = P_o \exp i(kr\cos\vartheta) \tag{3.2}$$

If the pressure scattered by an elastic boundary is denoted by P_{se}, then the resultant pressure for a thin shell becomes

$$P = P_i + P_{se} \tag{3.3}$$

The term P_{se} may be broken up into two components, a term P_{se_∞} which is the pressure scattered if the shell behaved like a rigid body, and another component P_r, i.e.

$$P_{sc} = P_{s\infty} + P_r \tag{3.4}$$

Therefore, the resultant pressure becomes

$$P = P_i + P_{s\infty} + P_r \tag{3.5}$$

From equation (1.6), the resultant pressure and velocity are related by

$$\frac{\partial P}{\partial n} = (i\omega\rho)\dot{w} \quad \text{on } S_o \tag{3.6}$$

where the resultant velocity on S_o is

$$\dot{w} = (\dot{w}_i + \dot{w}_{s\infty}) + \dot{w}_r \tag{3.7}$$

Substituting for w and P in the above, yields the four relations

$$\begin{aligned} &\dot{w} = \dot{w}_r \quad \text{(a)} \qquad \dot{w}_i + \dot{w}_{s\infty} = 0 \quad \text{(b)} \\ &\dot{w}_r = \frac{-i}{\omega\rho}\frac{\partial P_r}{\partial n} \quad \text{(c)} \qquad \dot{w}_i = \frac{-i}{\omega\rho}\frac{\partial P_i}{\partial n} \quad \text{(d)} \end{aligned} \tag{3.8}$$

In order to apply the Helmholtz integral equation solution, the scattered velocity components are represented in the form

$$\dot{w}_{s\infty} = \sum_{n=o}^{\infty} W_n^{s\infty} P_n(\cos\theta), \qquad \dot{w}_r = \sum_{n=o}^{\infty} W_n^r P_n(\cos\theta) \tag{3.9}$$

The incident wave may be represented in terms of a series of concentric spherical waves as

$$P_i(r,\theta) = P_o \sum_{n=o}^{\infty} [(2n+1)(i)^n j_n(kr)] P_n(\cos\theta) \tag{3.10}$$

where $j_n(kr)$ is the spherical Bessel function. From equations (3.8b, d), the coefficients of $w_{s\infty}$ may be obtained, i.e.

$$W_n^{s\infty} = (iP_o/\rho c)(2n+1)(i)^n j_n'(ka) \tag{3.11}$$

In order to apply the Helmholtz integral equation solution, $P_{s\infty}$ is regarded as the pressure radiated by a spherical source vibrating with velocity $w_{s\infty}$ therefore

$$P_{s_\infty}(r,\vartheta) = i(\rho c)\sum_{n=0}^{\infty} \dot{W}_n^{s_\infty} P_n(\cos\vartheta)\,\frac{h_n(kr)}{h_n'(ka)}$$
$$= -P_o\sum_{n=0}^{\infty}(2n+1)(i)^n j_n'(ka)\,P_n(\cos\vartheta)\,\frac{h_n(kr)}{h_n'(ka)} \qquad (3.12)$$

The Helmholtz integral equation solution can also be used to determine P_r. Equation (3.8c) indicates that P_r has the nature of a radiated pressure caused by a spherical body vibrating with velocity w_r. This vibration is due to the elastic structure responding to the surface pressure generated by the incident wave field. This surface pressure may be written as

$$P_a(\vartheta) = P_i(a,\vartheta) + P_{s_\infty}(a,\vartheta)$$
$$= \sum_{n=0} f_n^a P_n(\cos\vartheta) \qquad (3.13)$$

where from equation (3.10) and (3.12)

$$f_n^a = \frac{P_o(2n+1)(i)^{n+1}}{(ka)^2 h_n'(ka)} \qquad (3.14)$$

From equation (2.30) in the previous chapter, the modal velocity W_n caused by the modal excitation f_n^a is

$$\dot{W}_n = \frac{-f_n^a}{z_n + Z_n} \qquad (3.15)$$

Thus

$$\dot{w}_r = -P_o\sum_{n=0}^{\infty}\frac{(2n+1)(i)^{n+1}}{(z_n+Z_n)(ka)^2\,[h_n'(ka)]}\,P_n(\cos\vartheta) \qquad (3.16)$$

From the Helmholtz solution, the radiated pressure P_r is

$$P_r(r,\vartheta) = i(\rho c)\sum_{n=0}^{\infty}\dot{W}_n^r P_n(\cos\vartheta)\,\frac{h_n(kr)}{h_n'(ka)} \qquad (3.17)$$

Substituting for W_n^r yields

$$P_r(r,\vartheta) = (\rho c)\, P_o \sum_{n=o}^{\infty} \frac{(2n+1)(i)^n h_n(kr)}{(z_n + Z_n)[(ka)h_n'(ka)]^2} P_n(\cos\vartheta) \qquad (3.18)$$

When r is a long distance from the boundary S_o, i.e. "far-field", the Hankel function $h_n(kr)$ may be approximated by

$$\frac{+1}{kr} \exp(ikr)(-i)^{n+1}$$

and the scattered pressure fields become

$$P_{s\infty}(r,\vartheta) = \frac{iP_o}{kr} \exp i(kr) \sum_{n=o}^{\infty} \frac{(2n+1)P_n(\cos\vartheta) j_n'(ka)}{h_n'(ka)} P_n(\cos\vartheta) \qquad (3.19)$$

$$P_r(r,\vartheta) = \frac{-i(\rho c)P_o}{kr} \exp i(kr) \sum_{n=o}^{\infty} \frac{(2n+1)P_n(\cos\vartheta)}{(z_n + Z_n)[(ka)h_n'(ka)]^2} \qquad (3.20)$$

4. *Methods of Presenting Scattering Solutions*

To examine the scattering behaviour of a thin elastic spherical shell, certain parameters for the scattering body need to be determined. These parameters include (i) the resultant pressure field in the backscatter direction, (ii) the backscattering cross-section of the target, (iii) the target strength of the scatterer, (iv) the reflection factor around the scattering body and (v) the intensity field around the scatterer. To determine these parameters, values previously given in chapter 2 for the properties of the shell and the propagation medium are used.

4.1 *Resultant Pressure Field in Front of Scatterer*

In this report, the resultant pressure magnitude in the backscatter direction is computed. This pressure field (normalized with respect to the incident pressure wave amplitude) may be written as

$$\hat{P} = |P|/P_o = |(P_i/P_o) + (P_{s\infty}/P_o) + (P_r/P_o)| \tag{4.1}$$

where the incident and elastic scattered pressures close to the sphere have been determined previously to be

$$P_i/P_o = P_i^N(r,\vartheta)/P_o = \exp(\hat{i}\tau r\cos\vartheta) \tag{4.3}$$

$$P_{s\infty}^N/P_o = P_{s\infty}^N(r,\vartheta)/P_o = -\sum_{n=0}^{\infty}(2n+1)(i)^n P_n(\cos\vartheta)\left[\frac{j_n'(\tau)}{h_n'(\tau)}\right]h_n(\tau\hat{r}) \tag{4.3}$$

$$P_r^N/P_o = P_r^N(r,\vartheta)/P_o = -(\rho c)\sum_{n=0}^{\infty}\frac{(2n+1)(i)^n P_n(\cos\vartheta)h_n(\tau\hat{r})}{(z_n+Z_n)[(\tau)h_n'(\tau)]^2} \tag{4.4}$$

where $\Omega_n^{(1)}$, $\Omega_n^{(2)}$ depend on β^2, ν, λ_n and

$$\tau = ka,\ \hat{r} = r/a,\ \psi = h/a,\ \Omega = \tau(c/c_p),\ \beta^2 = \psi^2/12,\ \lambda_n = n(n+1) \tag{4.5}$$

$$z_n = i(\rho c)\frac{h_n(\tau)}{h_n'(\tau)},\ Z_n = -i(\rho_s c_p)\left(\frac{\psi}{\Omega}\right)\frac{[\Omega^2-(\Omega_n^{(1)})^2][\Omega^2-(\Omega_n^{(2)})^2]}{[\Omega^2-(1+\beta^2)(\nu+\lambda_n-1)]} \tag{4.6}$$

4.2 *Resonance Scattering Theory*

The resonance scattering theory is applied in order to analyse the backscattering cross-section of a spherical shell. The backscattering cross-section is defined as the ratio of the scattered power (referred to a distance of 1 metre), to the intensity incident on a unit volume [8], and may be written as

$$\sigma = 4\pi\left|\frac{P_{se}(1,\pi)}{P_o}\right|^2 \tag{4.7}$$

Upon normalizing this cross section with respect to value πa^2, the form function $f(\pi)$ may be defined, i.e.

$$\frac{\sigma}{\pi a^2} = \left|\frac{2P_{se}(a,\pi)}{P_o}\right|^2 = |f(\pi)|^2 \tag{4.8}$$

where

$$f(\pi) = \sum_{n=0}^{\infty} f_n$$

and f_n is termed the n^{th} "partial wave". The form function may be broken up into two components; the backgrounds and the resonances, i.e.

$$|f(\pi)| = |f_{s\infty}(\pi) + f_r(\pi)| = |\sum_{n=0}^{\infty} f_{ns\infty} = \sum_{n=0}^{\infty} f_{nr}| \tag{4.9}$$

where $f_{ns\infty}$ and f_{nr} are the modal components and

$$|f_{s\infty}(\pi)| = |\frac{2p_{s\infty}(a,\pi)}{P_o}| = |(2i)\sum_{n=0}^{\infty} \frac{(2n+1)(-1)^n j_n'(\tau)}{\tau h_n'(\tau)}| \tag{4.10}$$

$$|f_r(\pi)| = |\frac{2P_r(a,\pi)}{P_o}| = |-(2i\rho c)\sum_{n=0}^{\infty} \frac{(2n+1)(-1)^n}{(z_n+Z_n)\tau^3 h_n'(\tau)^2}| \tag{4.11}$$

The resonance scattering theory is useful in the treatment of penetrable scatterers in that it establishes connections between the background and resonance features observable in the backscattering cross-section of any target.

4.3 *Target Strength*

The target strength in the far-field may be defined as

$$\begin{aligned} TS &= 20\log_{10}\left[|\frac{r[P^F_{s\infty}(r,\vartheta)+P^F_r(r,\vartheta)]}{P_o}|\right]_{\vartheta=180^\circ} \\ &= 20\log_{10}[(r/P_o)|P^F_{s\infty}(r,\vartheta)+P^F_r(r,\vartheta)|]_{\vartheta=180^\circ} \end{aligned} \tag{4.12}$$

where $P^F_{s\infty}$ P^F_r combine to give the scattered pressure in the far-field and

$$(r/P_o)P^F_{s\infty}(r,\vartheta) = (ia/\tau)\exp(i\tau\hat{r})\sum_{n=0}^{\infty}(2n+1)P_n(\cos\vartheta)[j_n'(\tau)/h_n'(\tau)] \tag{4.13}$$

$$(r/P_o)P^F_r(r,\vartheta) = -(ia/\tau)(\rho c)\exp(i\tau\hat{r})\sum_{n=0}^{\infty}\frac{(2n+1)P_n(\cos\vartheta)}{(z_n+Z_n)[(\tau)h_n'(\tau)]^2} \tag{4.14}$$

4.4 *Reflection Factor*

Using the expressions in the previous section, the ratio of scattered to incident pressure may be written as

$$\frac{P_{s\infty}^{F} + P_{r}^{F}}{P_{i}} = \frac{a}{r} e^{ika(1-\cos\vartheta)} f(\vartheta) \tag{4.15}$$

The $1/r$ term characterizes the spreading of the scattered wave, whilst the exponential term takes into account the phases of the incident and scattered waves. The reflection factor can be made independent of these terms by defining it as

$$R = (r/a) \left| e^{-ika(1-\cos\vartheta)} [(P_{s\infty}^{F} + P_{r}^{F})/P_{i}] \right| \tag{4.16}$$

to yield

$$R = \left| (i/\tau) \sum_{n=0}^{\infty} \frac{(2n+1)P_{n}(\cos\vartheta)}{h_{n}'(\tau)} \left[j_{n}'(\tau) - \frac{\rho c}{(\tau)^{2} h_{n}'(\tau)(z_{n} + Z_{n})} \right] \right| \tag{4.17}$$

The reflection factor will be computed as a function of angle around the body, for various *ka* values.

4.5 *Intensity Field Around Scatterer*

Using the solution to the resultant pressure field, the construction of two different types of time-averaged intensity plots are possible, including:

(a) Plots of the intensity magnitude around the body (both "near-field" and "far-field")

(b) Plots of the intensity vector field around the body ("near-field" only)

For both type (a) and (b) plots, the intensities for the scattered and resultant pressure fields are computed. The radial and transverse components of the intensity vector (averaged over one period of the wave) are defined as

$$I_{r}(r,\vartheta) = \frac{1}{2} Re[P(r,\vartheta)\dot{u}_{r}^{*}(r,\vartheta)] \tag{4.18}$$

$$I_{\vartheta}(r,\vartheta) = \frac{1}{2} Re[P(r,\vartheta)\dot{u}_{\vartheta}^{*}(r,\vartheta)] \tag{4.19}$$

where *Re* denotes the real part, * the complex conjugate and u_r, u_ϑ the velocity components corresponding to the pressure field P whether it be a scattered or resultant pressure. The magnitude and direction of the intensity vector are given by the formulae

$$\begin{aligned} I &= [I_r^2(r,\vartheta) + I_\vartheta^2(r,\vartheta)]^{1/2} \\ \phi &= \vartheta + \arctan[I_\vartheta(r,\vartheta)/I_r(r,\vartheta)] \\ \vartheta &= \arctan[z/x], \quad r = [x^2+z^2]^{1/2} \end{aligned} \tag{4.20}$$

where x, z are shown in Figure 1. For the polar intensity plots of type (a), the intensity value is first divided by the incident intensity $I_o = P_o^2/2\rho c$. The intensity is then normalized with respect to the maximum value that it obtains over the range of angles from 0° to 360°. For the type (b) intensity vector plots, each vector has first been divided by I_o, and then normalized with respect to the magnitude of the largest vector in the plot. The square root of the magnitude is then calculated and multiplied by the grid spacing. The vectors are plotted over the coordinate range $-2 \le (x/a) \le 2$ and $0 \le (z/a) \le 2$, where a is the mean radius of the spherical scatterer.

In order to compute the time-averaged intensity, the velocity field associated with the pressure field must be found. This may be determined from Euler's equation, $\nabla P = (i\omega\rho)u$, or in component form

$$\dot{u}_r = \left(\frac{1}{\rho c}\right)\left(\frac{-i}{k}\right)\frac{\partial P}{\partial r}, \quad \dot{u}_\vartheta = \left(\frac{1}{\rho c}\right)\left(\frac{-i}{kr}\right)\frac{\partial P}{\partial \vartheta} \tag{4.21}$$

Using the "near-field" and "far-field" pressure expressions given in sections 4.1 and 4.2, the following velocity components are obtained.

Velocity due to incident pressure P_i

$$(\rho c/P_o)[\dot{u}_r]_i = +\cos\vartheta \exp(ikr\cos\vartheta) \tag{4.22}$$

$$(\rho c/P_o)[\dot{u}_\vartheta]_i = -\sin\vartheta \exp(ikr\cos\vartheta) \tag{4.23}$$

Velocity due to rigid scattered pressure $P_{s\infty}$

Near-field:

$$(\rho c/P_o)[\dot{u}_r^N]_{s\infty} = \sum_{n=0}^{\infty} (2n+1)(i)^{n+1} P_n(\cos\vartheta) \frac{j_n'(\tau)}{h_n'(\tau)} h_n'(\tau\hat{r}) \tag{4.24}$$

$$(\rho c)/P_o)[\dot{u}_\vartheta^N]_{s\infty} = -(\sin\vartheta/\tau\hat{r}) \sum_{n=o}^{\infty} (2n+1)(i)^{n+1} P_n'(\cos\vartheta) \frac{j_n'(\tau)}{h_n'(\tau)} h_n(\tau\hat{r}) \tag{4.25}$$

Far-field:

$$(\rho c/P_o)[\dot{u}_r^F]_{s\infty} = (i/\tau\hat{r})e^{i\tau\hat{r}} \sum_{n=o}^{\infty} (2n+1)P_n(\cos\vartheta) \frac{j_n'(\tau)}{h_n'(\tau)} \tag{4.26}$$

$$(\rho c/P_o)[\dot{u}_\vartheta^F]_{s\infty} = (-\sin\vartheta/(\tau\hat{r})^2)e^{i\tau\hat{r}} \sum_{n=o}^{\infty} (2n+1)P_n'(\cos\vartheta) \frac{j_n'(\tau)}{h_n'(\tau)} \tag{4.27}$$

Velocity due to the radiated pressure P_r

Near-field:

$$(1/P_o)[\dot{u}_r^N] = \sum_{n=o} \frac{(2n+1)(i)^{n+1} P_n(\cos\vartheta)h_n'(\tau\hat{r})}{(z_n + Z_n)[(\tau)h_n'(\tau)]^2} \tag{4.28}$$

$$(1/P_o)[\dot{u}_\vartheta^N] = -(\sin\vartheta/\tau\hat{r}) \sum_{n=o}^{\infty} \frac{(2n+1)(i)^{n+1} P_n'(\cos\vartheta)h_n(\hat{\tau}r)}{(z_n + Z_n)[(\tau)h_n'(\tau)]^2} \tag{4.29}$$

Far-field:

$$(1/P_o)[\dot{u}_r^F] = (-i/\tau\hat{r})e^{i\tau\hat{r}} \sum_{n=o}^{\infty} \frac{(2n+1)P_n(\cos\vartheta)}{(z_n + Z_n)[(\tau)h_n'(\tau)]^2} \tag{4.30}$$

$$(1/P_o)[\dot{u}_\vartheta^F] = (\sin\vartheta/(\tau\hat{r})^2)e^{i\tau\hat{r}} \sum_{n=o} \frac{(2n+1)P_n'(\cos\vartheta)}{(z_n + Z_n)[(\tau)h_n'(\tau)]^2} \tag{4.31}$$

By combining equations (2.1), (2.17) and (3.16), the radial and tangential displacements are derived, i.e.

$$w(\vartheta) = A_o \sum_{n=o}^{\infty} \frac{(2n+1)(i)^n P_n(\cos\vartheta)}{(Z_n + z_n) h_n'(\tau)} \tag{4.32}$$

$$u(\vartheta) = A_o \sum_{n=o}^{\infty} \frac{\alpha_n (2n+1)(i)^n (1-\cos^2\vartheta)^{1/2} P_n'(\cos\vartheta)}{(Z_n + z_n) h_n'(\tau)} \tag{4.33}$$

where

$$A_o = \frac{P_o}{\omega(\tau)^2}, \quad \alpha_n = \frac{-[\beta^2(\nu + \lambda_n - 1) + (1+\nu)]}{[\Omega^2 - (1+\beta^2)(\nu + \lambda_n - 1)]} \tag{4.34}$$

Using equations (4.32) and (4.33), the deformed shape of the elastic shell may be plotted.

5. *Results and Discussion*

In this chapter, plots of the various scattering parameters for the elastic spherical shell are discussed and compared with those of the rigid sphere. For some plots, only four specific *ka* values will be considered, namely *ka* = 1.14, 1.44, 3.30 and 5.20. These values correspond to the n = 2, 3 resonances, as well as a dip and a maximum in the target strength spectrum.

5.1 *Resultant Pressure Field*

Figures 2(a) to 2(d) show the normalized resultant pressure as a function of r/a for the above four *ka* values. For Figures (a) and (b), corresponding to the n = 2, 3 resonances of the shell, radiation scattering far outweighs that of rigid body scattering, resulting in the shell pressure being many times that of its rigid sphere counterpart. In Figure (c) away from the surface, the radiation scattering and rigid scattering interfere destructively thus cancelling each others' effect, whilst for Figure (d) the shell pressure magnitude is comparable to that of the rigid sphere except for a phase difference of approximately 180°.

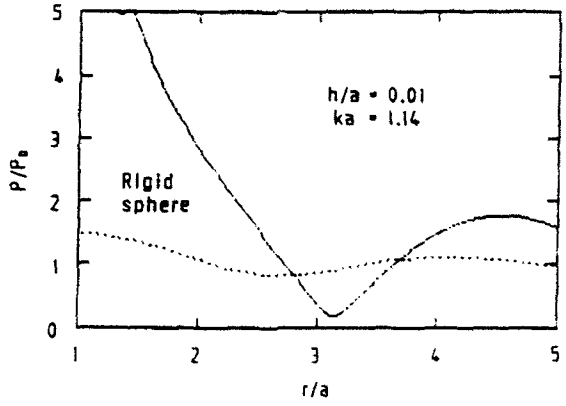

Figure 2(a): Resultant Pressure in front of Elastic Shell

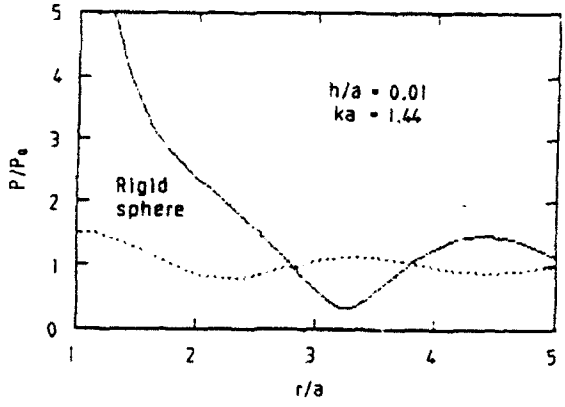

Figure 2(b): Resultant Pressure in front of Elastic Shell

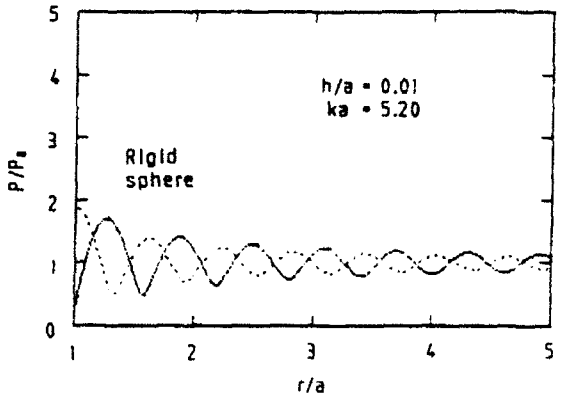

Figure 2(c): Resultant Pressure in front of Elastic Shell

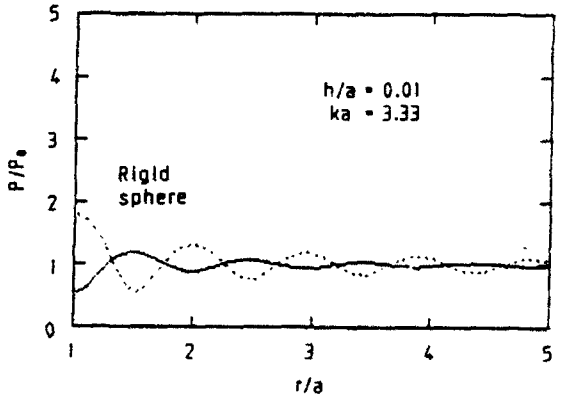

Figure 2(d): Resultant Pressure in front of Elastic Shell

5.2 *Resonant Scattering Theory*

As mentioned previously, each partial wave contained in the form function of a penetrable scatterer can be broken up into two components, a smooth background, and a set of modal resonances. Figures 3(a,b) show the first five modal backgrounds and modal resonances for the thin steel spherical shell.

The frequency dependence of the form function contains effects which arise from four distinct types of contributions. These contributions are (1) specular reflection, (2) creeping waves, (3) symmetric and antisymmetric Lamb waves and (4) waves bouncing within the inner and outer boundaries of the shell material.

Specular reflection, which is effectively the rigid body reflection, does not produce any drastic change in the form function since these waves do not travel along any part of the surface. Creeping waves are diffracted waves that originate at the edge of the shadow boundary and reradiate in all directions as they circumnavigate the body in the fluid medium. Extrema in the form function due to waves scattered within the elastic boundaries, can only occur for high frequencies.

Background

The background is essentially the rigid body scattering response, i.e. the response of the scatterer as if it were impenetrable, and is due to creeping waves travelling around the shell. The background is the contribution due to the scatterers' shape only, and is thus independent of changes in shell thickness and material composition.

Modal Resonances

The set of modal resonances is the radiation scattering response, and represents the sound radiation from the shell which is undergoing forced vibrations due to the incident wave pressure. This energy of vibration in the shell goes into the creation of surface (Lamb) waves, and the resonances are the resultant process of phase reinforcement of the surface waves during the scattering process as they travel around the shell.

For thin shells such as the one considered in this study, only the zeroth order symmetric Lamb wave is dominant, and there is only one resonance per mode n (see Fig. 3(b)). The resulting form function has a simple structure as compared to that of thick shells, where many Lamb waves interact simultaneously, making the response difficult to interpret. Figure 4 shows the resultant backscattering cross-section for the steel spherical shell.

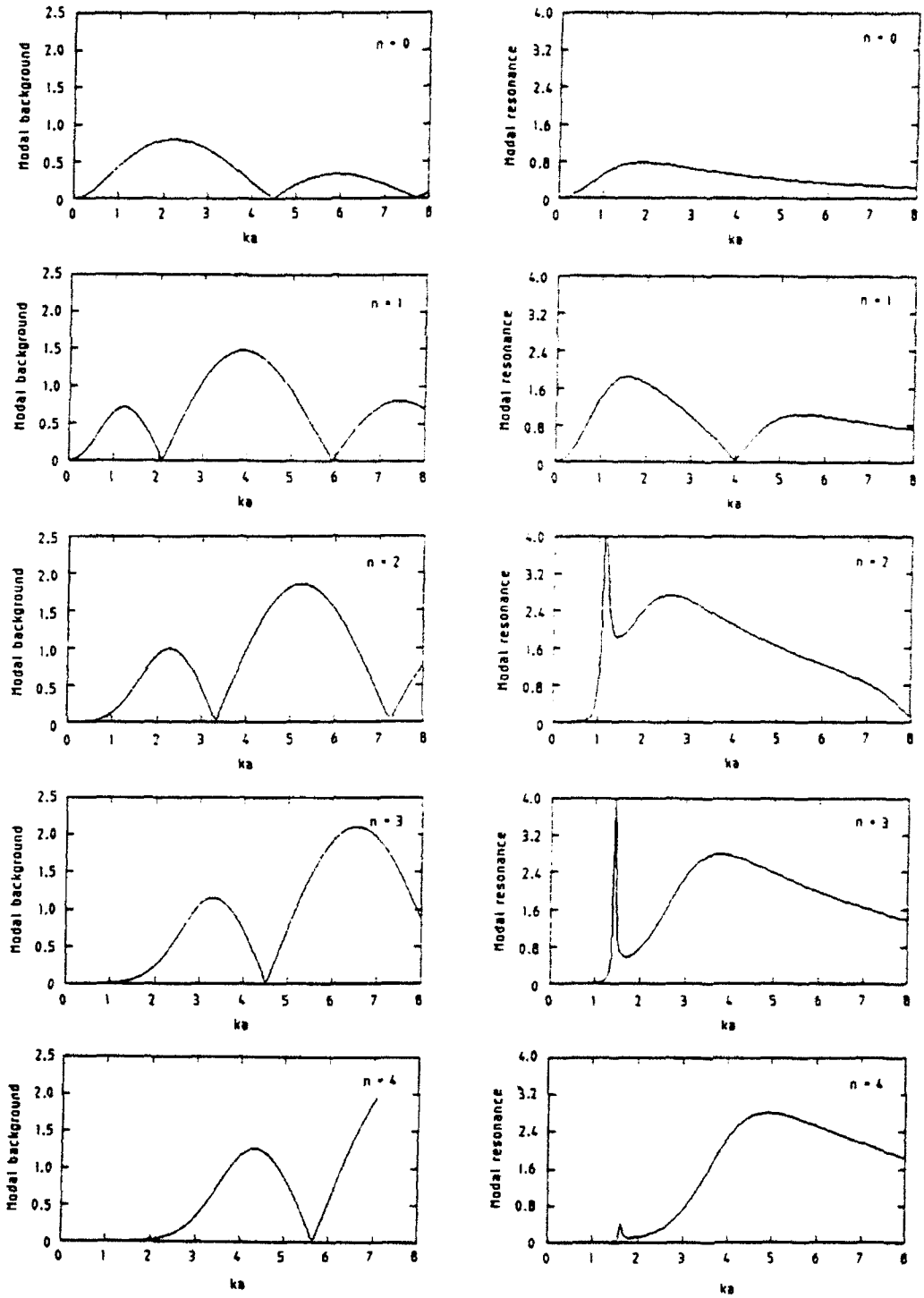

Figure 3: First five sets of (a) modal backgrounds and (b) modal resonances for a thin steel spherical shell.

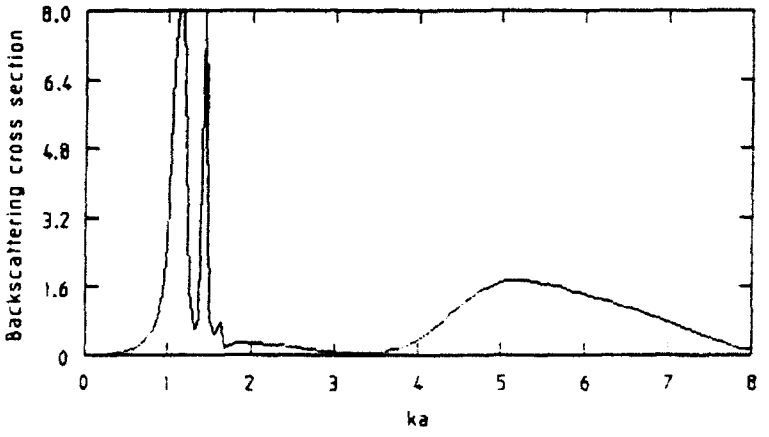

Figure 4: *Normalized Backscattering Cross-Section of a Thin Steel Spherical Shell.*

5.3 Target Strength

The monostatic target strength spectra of the thin shell, is illustrated in Figure 5, where the dominant resonant peaks are labelled by their individual modal numbers. The resonant peaks of this shell are high, with the $n = 2$ peak being almost 20 dB above the "rigid body" datum plot. The oscillations in the rigid sphere curve are the result of interference between the creeping waves and the specular reflection. There are no resonances for either the $n = 0$ or the $n = 1$ modes. The $n = 0$ mode which is termed the "breathing mode" corresponds to a uniform expansion and contraction of the spherical shell, which does not occur for plane wave ensonification. The $n = 1$ resonance occurs at zero frequency and corresponds to an undeformed shell moving back and forth in the fluid medium.

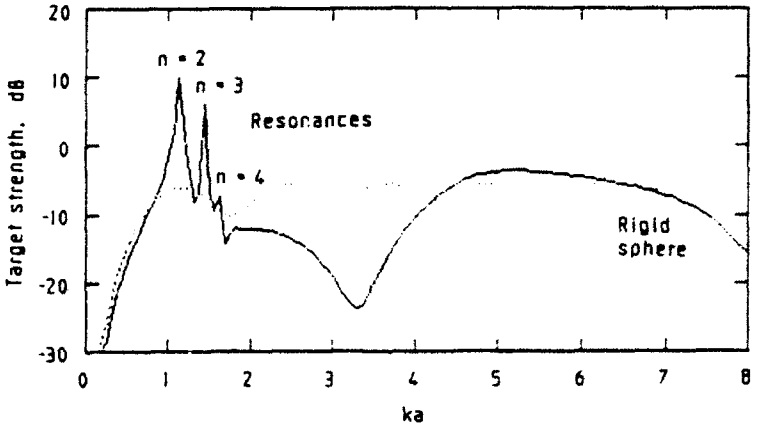

Figure 5: Monostatic Target Strength of an Elastic Shell.

5.4 Reflection Factor

Figures 6(a) to 6(d) show the reflection factor for the four *ka* values of interest. In Figure 6(a), the scattered field is symmetric about the plane containing the shadow boundary. In Figures 6(c) and 6(d) the overall appearance of the scattered field is not too different from that for a rigid sphere, where there is a strong beam of interfering radiation behind the sphere. There are however variations in the magnitude of the backscattered echo which do not occur with the rigid sphere at higher frequencies.

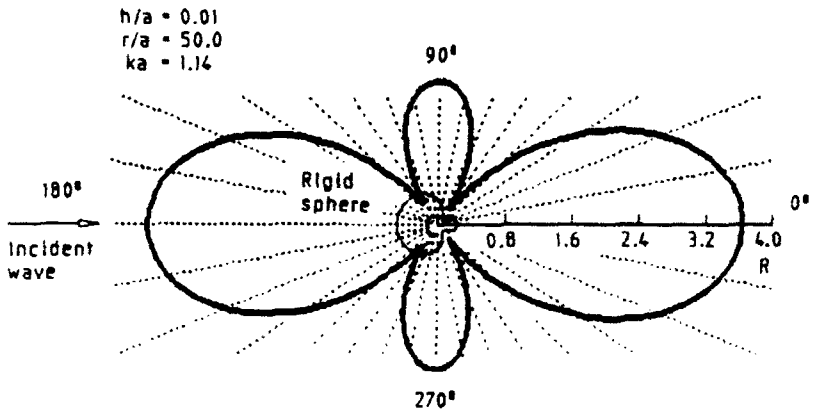

Figure 6(a): Reflection Factor for an Elastic Shell.

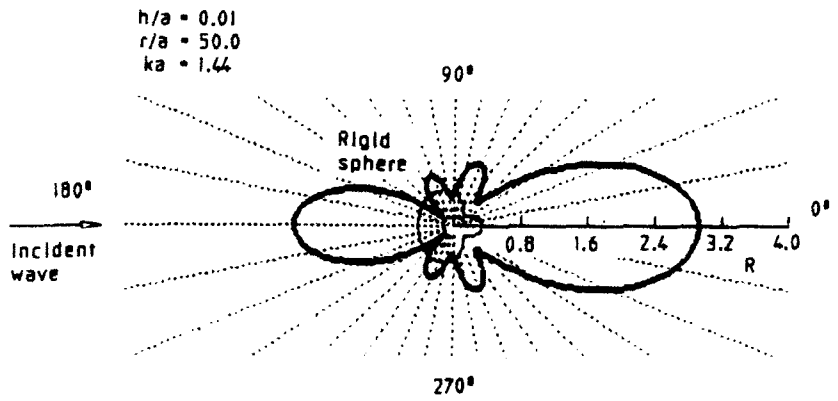

Figure 6(b): Reflection Factor for an Elastic Shell.

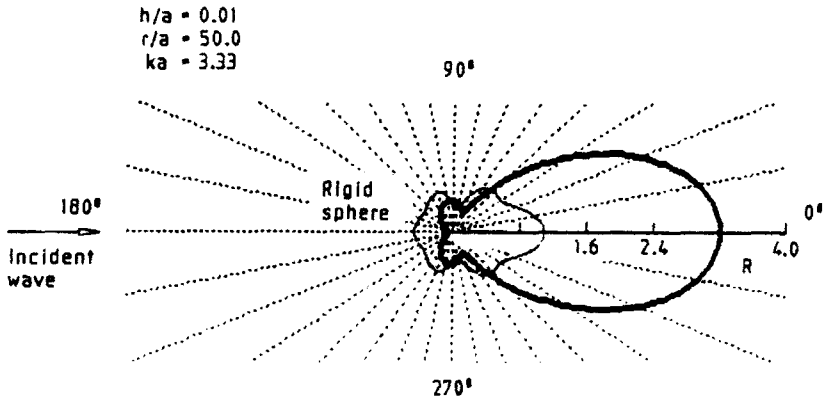

Figure 6(c): Reflection Factor for an Elastic Shell.

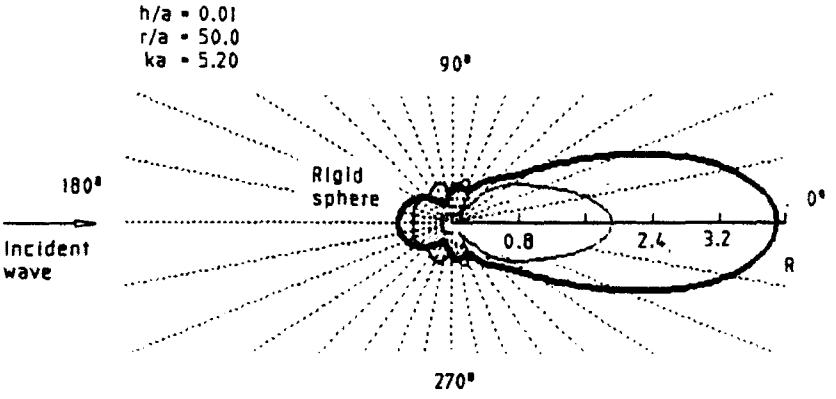

Figure 6(d): Reflection Factor for an Elastic Shell.

5.5 *Intensity*

Figures 7 and 9 display the scattered and resultant intensity magnitudes in the near field as a function of angle around the scatterer. The scattered response patterns in the far-field are shown in Figure 8.

The scattered and resultant intensity vector fields around the shell are shown in Figures 10 and 11. An examination of the resultant fields in Figures 11(a,b) clearly shows the large distortion of the incident sound field at the resonant frequencies. At $ka = 1.14$ ($n = 2$) there is a maximum of power flow into the shell at the poles, and a maximum of power flow out of the shell at the equator. At $ka = 1.44$ ($n = 3$) however, there is a minimum of power flow into the shell at the poles, but still a maximum of power flow out of the shell at the equator.

The resultant intensity vector fields which correspond to the non-resonant ka values 3.33 and 5.20 are shown in Figures 11(c,d). Unlike the previous resonant intensity fields which display complex variations in pattern, these fields are very similar to those generated by an impenetrable sphere. The deformed shapes of the shell at the four ka values is illustrated in Figures 12(a) to 12(d). These results apply to deformations which occur at various times during the excitation period and demonstrate the types of results which can be produced. It should be noted that the deformations as shown have been scaled by the factor $0.1\ a/[w(\vartheta)]_{max}$.

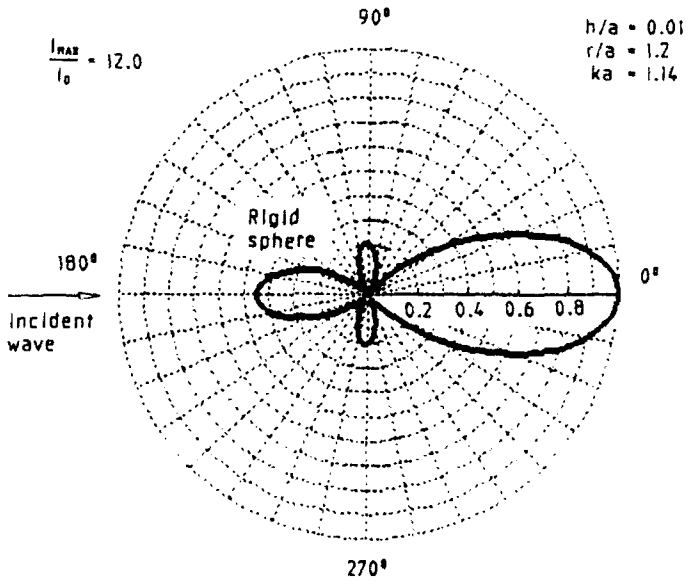

Figure 7(a): Scattered Intensity around an Elastic Shell.

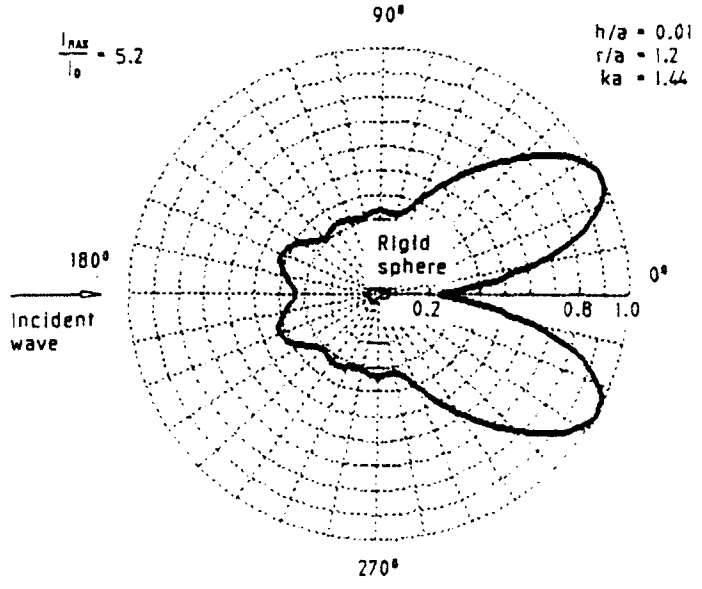

Figure 7(b): Scattered Intensity around an Elastic Shell.

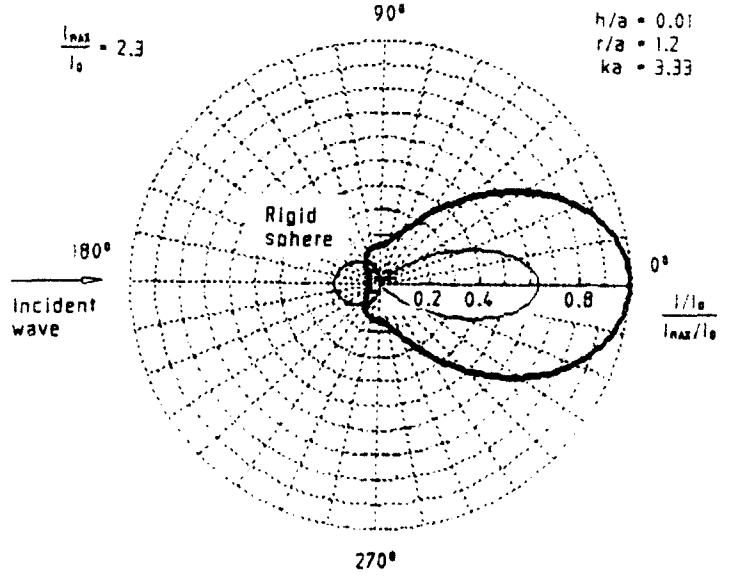

Figure 7(c): Scattered Intensity around an Elastic Shell.

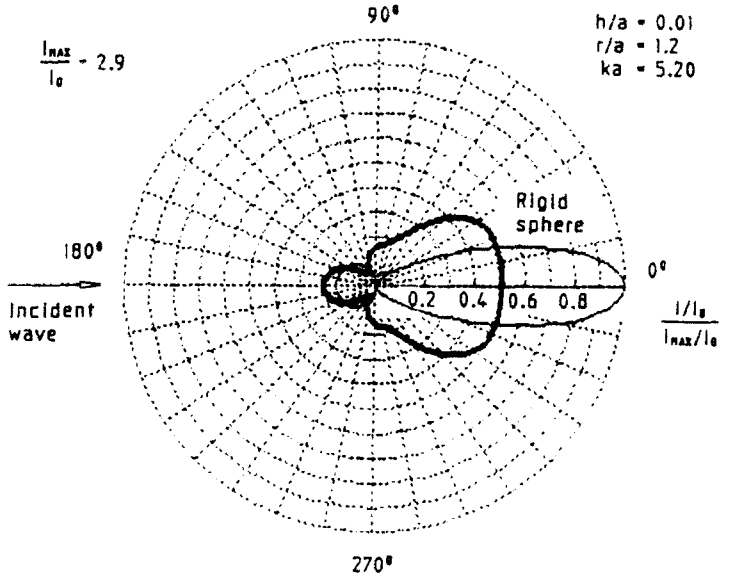

Figure 7(d): Scattered Intensity around an Elastic Shell.

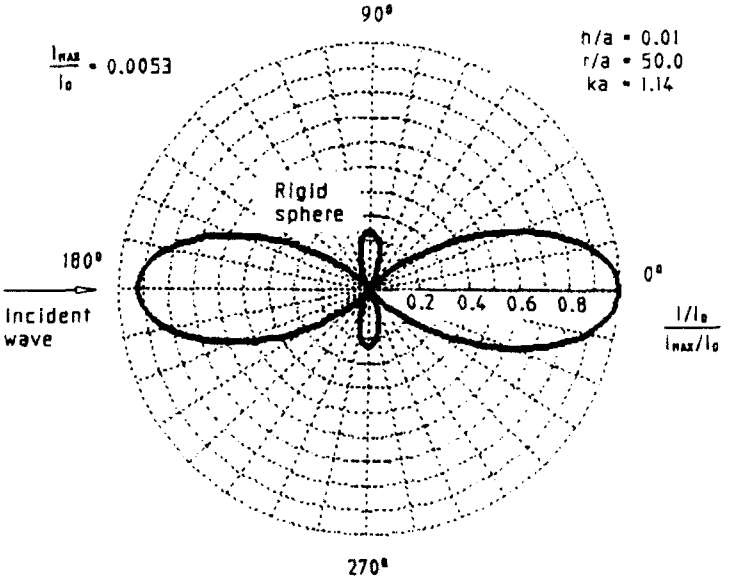

Figure 8(a): Scattered Intensity around an Elastic Shell.

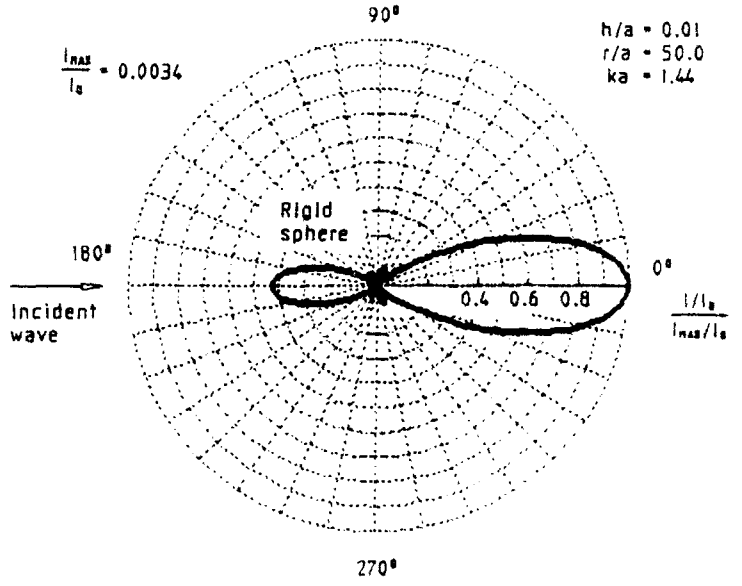

Figure 8(b): Scattered Intensity around an Elastic Shell.

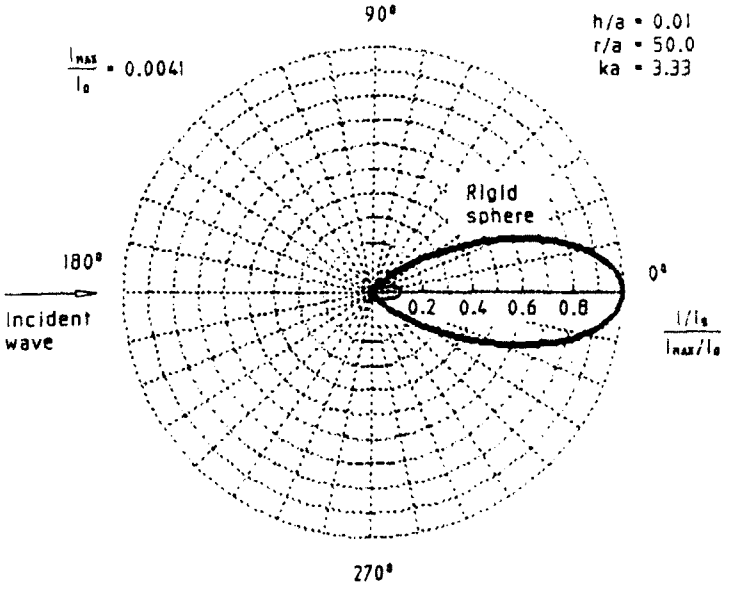

Figure 8(c): Scattered Intensity around an Elastic Shell.

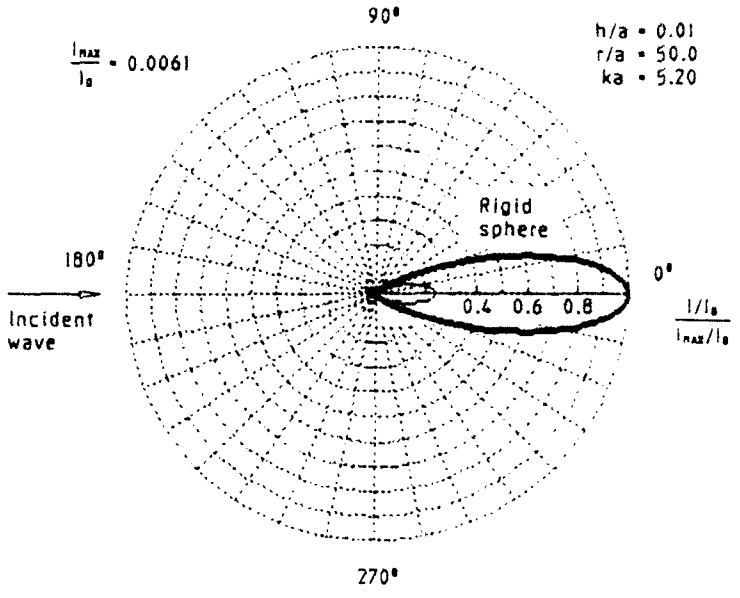

Figure 8(d): Scattered Intensity around an Elastic Shell.

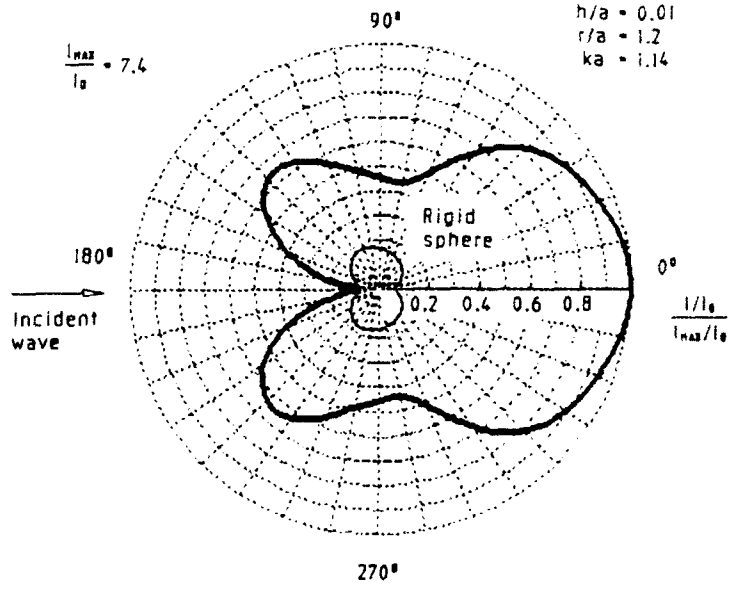

Figure 9(a): Resultant Intensity around an Elastic Shell.

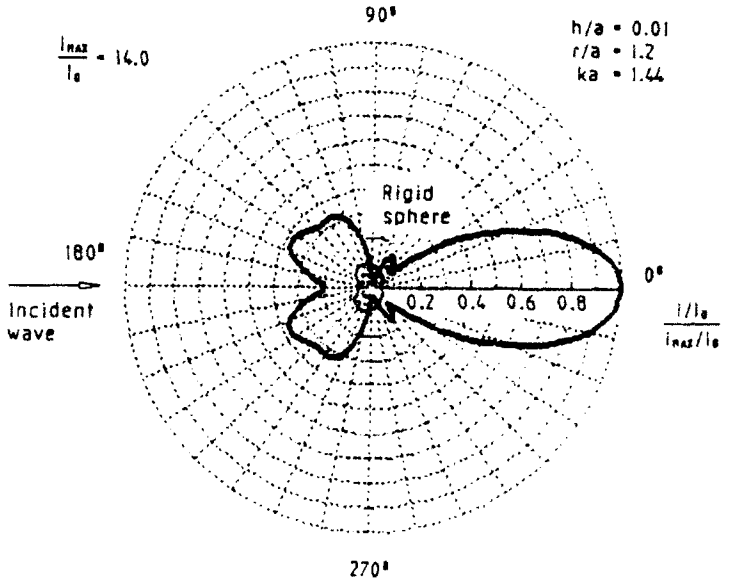

Figure 9(b): Resultant Intensity around an Elastic Shell.

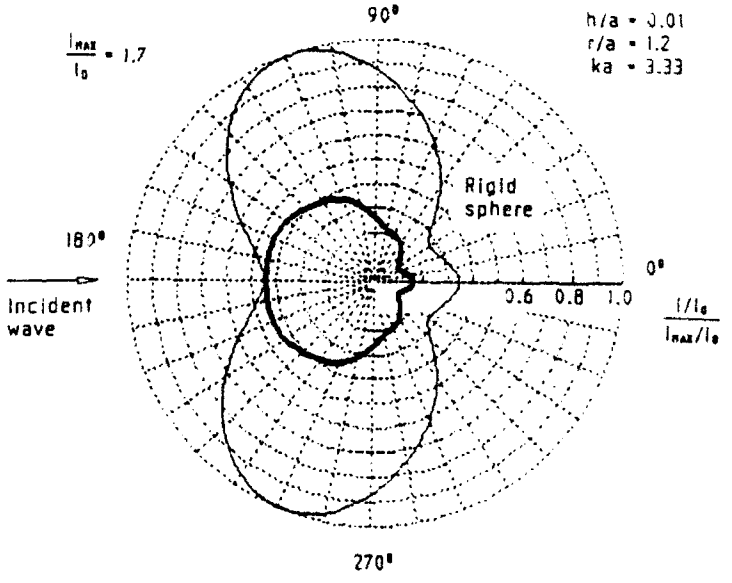

Figure 9(c): Resultant Intensity around an Elastic Shell.

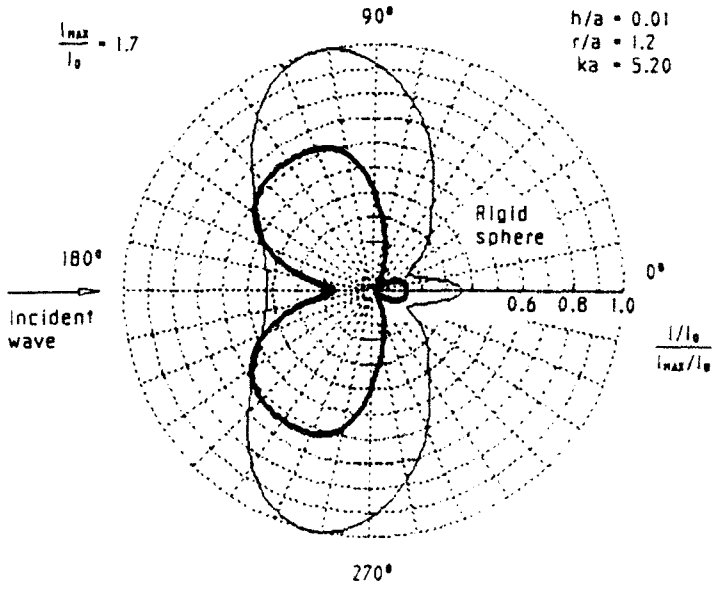

Figure 9(d): Resultant Intensity around an Elastic Shell.

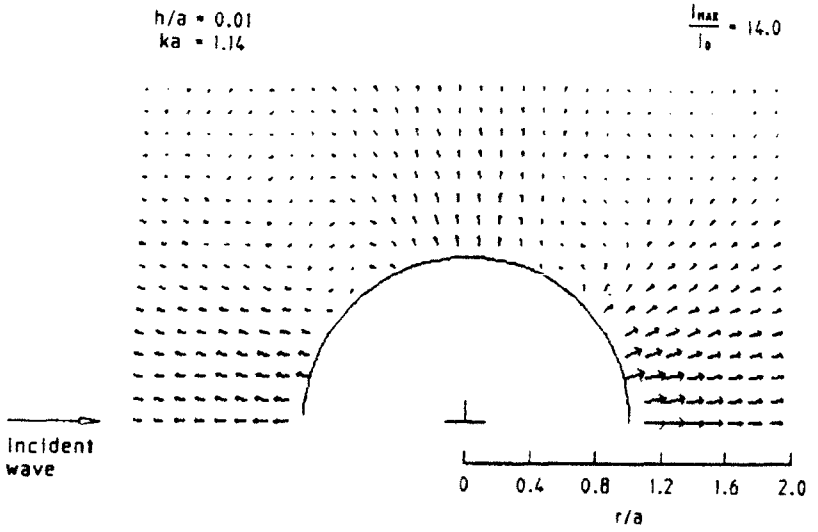

Figure 10(a): Scattered Intensity $[I/Imax]^{1/2}$ around an Elastic Shell.

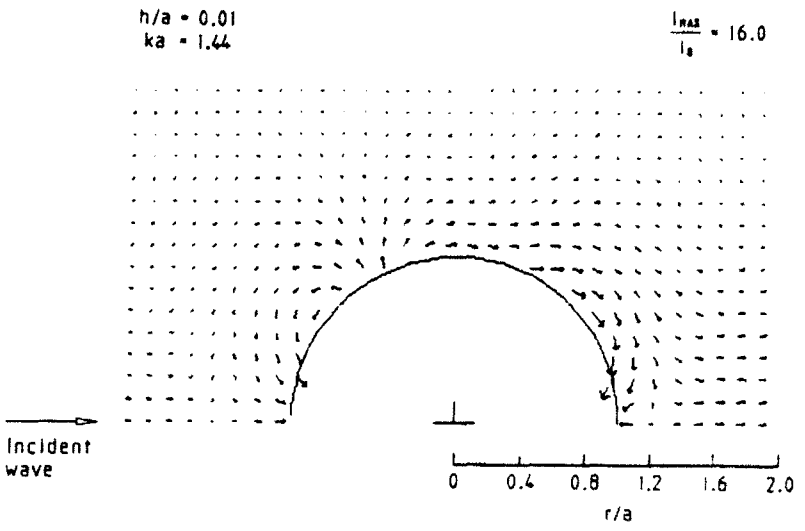

Figure 10(b): *Scattered Intensity $[I/Imax]^{1/2}$ around an Elastic Shell.*

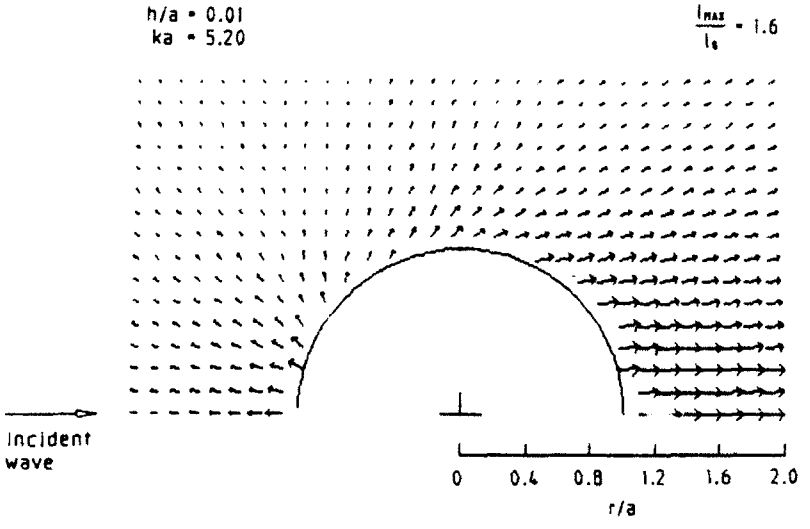

Figure 10(c): *Scattered Intensity $[I/Imax]^{1/2}$ around an Elastic Shell.*

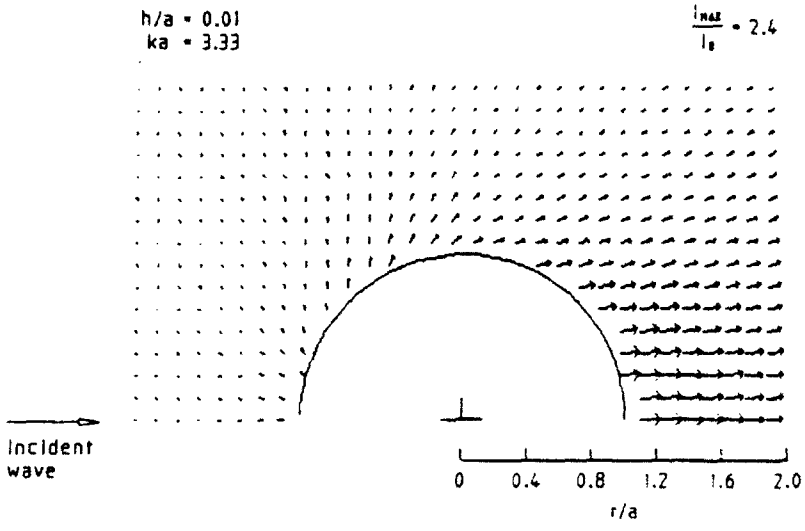

Figure 10(d): Scattered Intensity $[I/Imax]^{1/2}$ around an Elastic Shell.

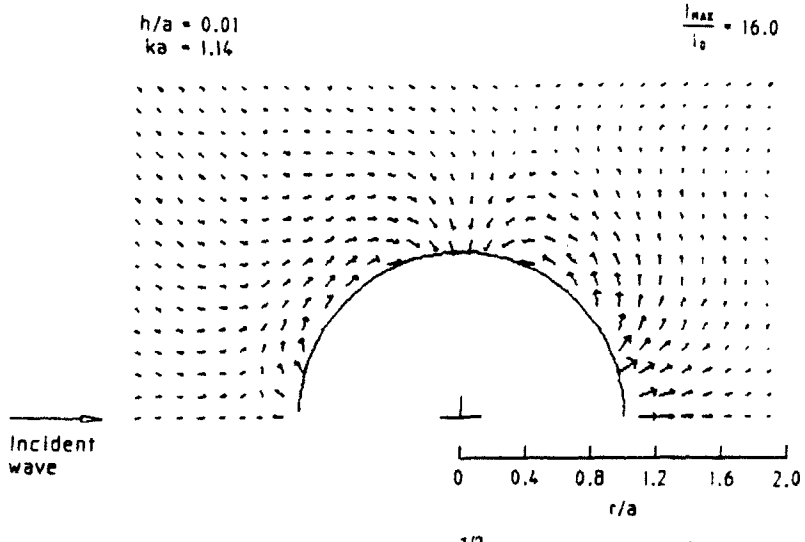

Figure 11(a): Resultant Intensity $[I/Imax]^{1/2}$ around an Elastic Shell.

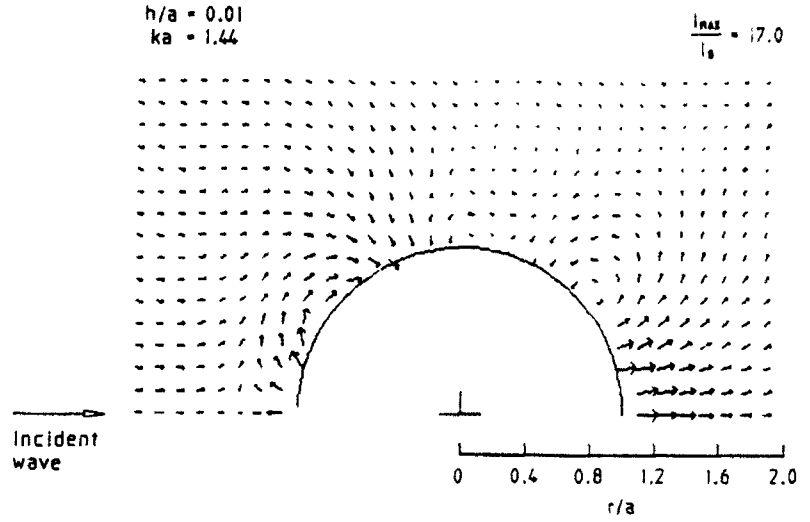

Figure 11(b): Resultant Intensity $[I/Imax]^{1/2}$ around an Elastic Shell.

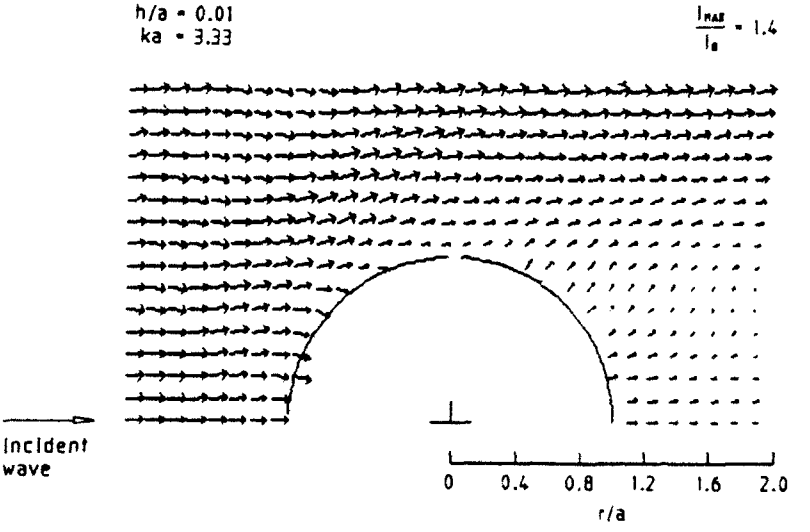

Figure 11(c): Resultant Intensity $[I/Imax]^{1/2}$ around an Elastic Shell.

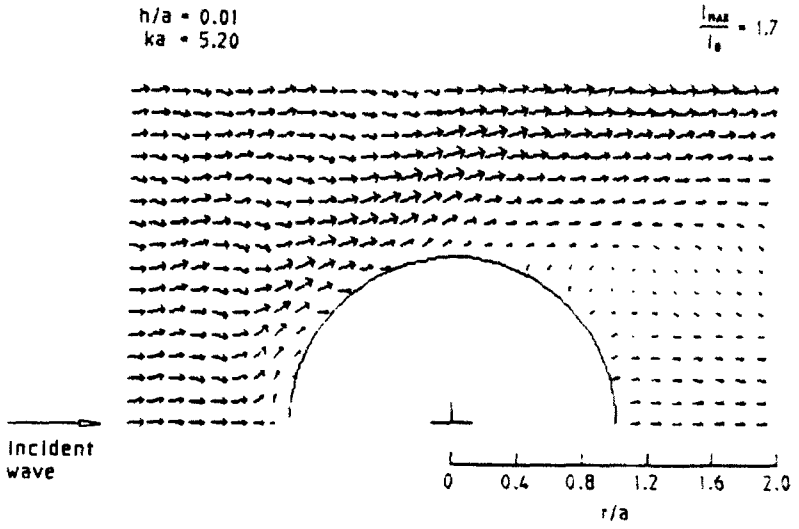

Figure 11(d): Resultant Intensity $[I/Imax]^{1/2}$ around an Elastic Shell.

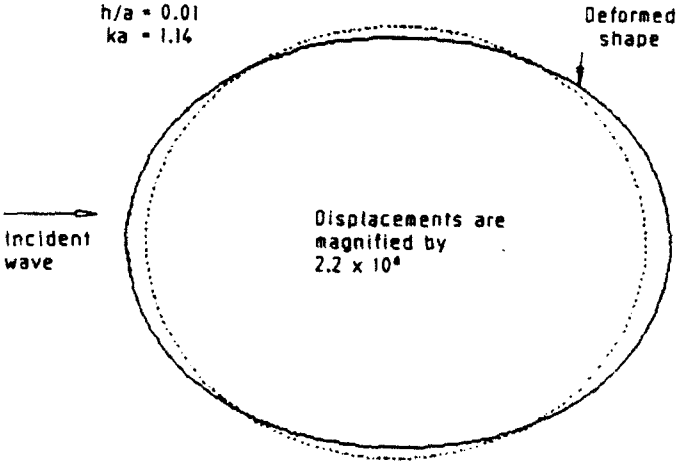

Figure 12(a): Deformed shape of elastic shell. (Incident pressure P_o = 10 Pa) (Scaling factor = 2.2 E+06).

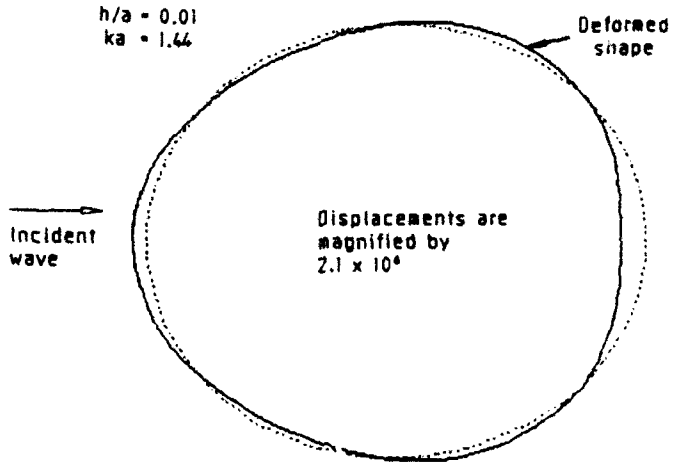

Figure 12(b): *Deformed shape of elastic shell. (Incident pressure P_o = 10 Pa) (Scaling factor = 2.1 E+06)*

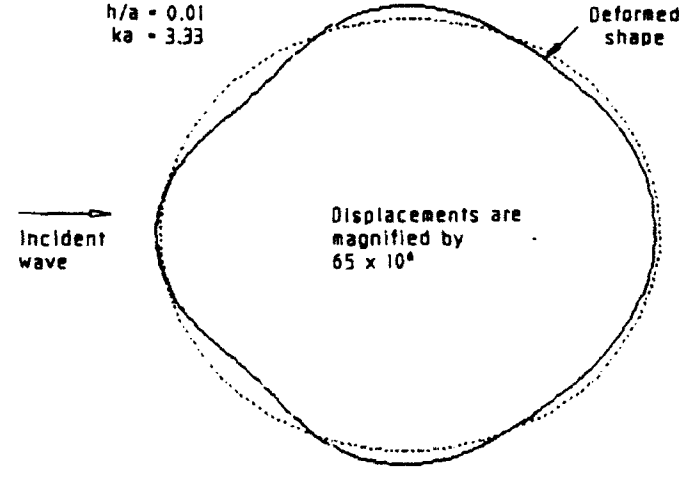

Figure 12(c): *Deformed shape of elastic shell. (Incident pressure P_o = 10 Pa) (Scaling factor = 6.5 E+07).*

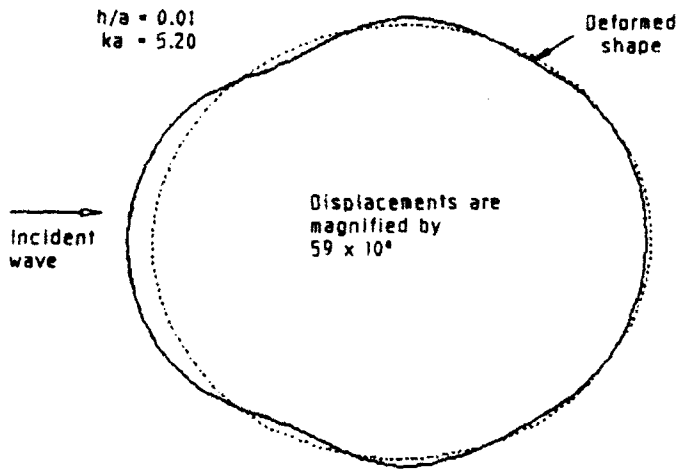

Figure 12(d): Deformed shape of elastic shell. (Incident pressure P_o = 10 Pa) (Scaling factor = 5.9 E+07).

6. Conclusion

An analysis of the plane wave scattering from a thin steel spherical shell submerged in water has been carried out and results are presented for *ka* values up to 8. Various scattering parameters such as target strength, back-scattering cross-section, reflection factor and the intensity field around the body have been computed to illustrate the solutions. Results from a rigid sphere of comparable size have also been included for comparison purposes. At values of *ka* corresponding to the shell resonances, intensity vector plots show large variations in the sound field around the shell and target strength results indicate echoes of up to 20 dB greater than that obtained from a similarly sized rigid sphere.

7. References

1. Partridge, C.J. (1990).
Sound wave scattering from a rigid sphere (MRL Technical Note in publication). Maribyrnong, Vic.: Materials Research Laboratory.

2. Junger, M.C. and Feit, D. (1972).
Sound, structures, and their interaction. MIT Press.

3. Skudrzyk, E. (1971).
The foundations of acoustics. Springer-Verlag Publishing Co Ltd.

4. Gaunard, G.C. and Werby, M.F. (1985).
Resonance response of submerged, acoustically excited thin and thick shells. *Journal of the Acoustical Society of America,* 77 (6).

5. Gaunard, G.C. and Werby, M.F. (1987).
Lamb and creeping waves around submerged spherical shells resonantly excited by sound scattering. *Journal of the Acoustical Society of America,* 82 (6).

6. Morse, P.M. and Ingard, K.U. (1972).
Theoretical acoustics. Princeton University Press.

7. James, J.H. (1984).
Intensity vectors of sound scattering by a spherical shell (AMTE(N) TM 84080). Teddington: Admiralty Marine Technology Establishment.

8. Urick, R.J. (1983).
Principles of underwater sound (3rd Edn.). McGraw-Hill Publishing Co Ltd.

Glossary of Symbols

P	Resultant pressure
P_o	Incident pressure amplitude
P_i	Incident pressure
P_{se}	Scattered pressure from an elastic body
$P_{s\infty}$	Scattered pressure from a rigid body (infinite impedance)
P_r	Radiated pressure from an elastic body
P_a	Pressure at the shell surface ($r = a$)
σ	Backscattering cross-section of target
$f(\pi)$	Form function in backscatter direction
$f_{n\infty}$, f_{nr}	Modal backgrounds and resonances of form function
I_o	Average intensity magnitude of the incident pressure
I_r, I_φ	Radial and tangential components of the intensity vector
$G(\mathbf{r} \mid \mathbf{r}_o)$	Green's function
ω	Angular frequency
Ω	Normalized frequency of incident pressure wave
$\Omega_n^{(i)}$	Natural frequencies of vibration for a spherical shell (i = 1, 2)
k	Acoustic wavenumber
a	Mean radius of spherical shell
c	Speed of sound in water
c_s	Speed of wave in a shell
ρ	Density of water
ρ_s	Density of shell material
E	Young's modulus of the shell
ν	Poisson's ratio of the shell
h	Shell thickness
β^2	Shell thickness factor
$\varepsilon_{\theta\theta}$, $\varepsilon_{\phi\phi}$	Spherical strains
$\sigma_{\theta\theta}$, $\sigma_{\phi\phi}$	Spherical stresses
r, θ, ϕ	Spherical coordinates
E_K	Kinetic energy
E_S	Strain energy
S_o	Boundary of sphere ($r = a$)
w	Normal velocity component of resultant pressure at S_o
w_i	Normal velocity component of incident pressure at S_o
$w_{s\infty}$	Normal velocity component of rigid scattered pressure at S_o
w_r	Normal radiated velocity component at S_o
$\mathbf{n}$	Unit outward normal
z_n	Modal acoustic impedance
Z_n	Modal mechanical impedance

SECURITY CLASSIFICATION OF THIS PAGE **UNCLASSIFIED**

DOCUMENT CONTROL DATA SHEET

REPORT NO.	AR NO.	REPORT SECURITY CLASSIFICATION
MRL-TR-91-10	AR-006-357	Unclassified

TITLE

Sound wave scattering from an elastic spherical shell

AUTHOR(S)
C.J. Partridge

CORPORATE AUTHOR
Materials Research Laboratory
PO Box 50
Ascot Vale Victoria 3032

REPORT DATE	TASK NO.	SPONSOR
January, 1993	NAV 89/020	RAN

FILE NO.	REFERENCES	PAGES
G6/4/8-4036	8	52

CLASSIFICATION/LIMITATION REVIEW DATE

CLASSIFICATION/RELEASE AUTHORITY
Chief, Underwater Systems Division

SECONDARY DISTRIBUTION

Approved for public release

ANNOUNCEMENT

Announcement of this report is unlimited

KEYWORDS

Wave Scattering
Acoustics
Sound Waves
Spherical Shell
Pressure Fields

ABSTRACT

The Helmholtz integral equation may be formulated by combining the scalar wave equation and Euler's equation for motion within a fluid. The solution to this integral equation yields the radiated pressure from a submerged vibrating body. The solution obtained from applying Hamilton's variational principle governs the response to a given surface pressure excitation. These two solutions may be used in conjunction to investigate the scattering of incident sound waves from shell-like bodies. In this report, the scattering from a submerged steel spherical shell having a thickness to radius ratio of 0.01 is investigated for *ka* values up to 8.

Sound Wave Scattering from an Elastic Spherical Shell

C.J. Partridge

(MRL-TR-91-10)

DISTRIBUTION LIST

Director, MRL
Chief, Maritime Operations Division
Dr C.I. Sach
C.J. Partridge
MRL Information Service

Chief Defence Scientist (for CDS, FASSP, ASSCM) (1 copy only)
Director, Surveillance Research Laboratory
Director (for Library), Aeronautical Research Laboratory
Director, Electronics Research Laboratory
Head, Information Centre, Defence Intelligence Organisation
OIC Technical Reports Centre, Defence Central Library
Officer in Charge, Document Exchange Centre (8 copies)
Army Scientific Adviser, Russell Offices
Air Force Scientific Adviser, Russell Offices
Navy Scientific Adviser, Russell Offices - data sheet only
Scientific Adviser, Defence Central
Director-General Force Development (Land)
Senior Librarian, Main Library DSTOS
Librarian, MRL Sydney
Librarian, H Block
UK/USA/CAN ABCA Armies Standardisation Rep. c/- DGAT (8 copies)
Librarian, Australian Defence Force Academy
Counsellor, Defence Science, Embassy of Australia - data sheet only
Counsellor, Defence Science, Australian High Commission - data sheet only
Scientific Adviser to DSTC, C/- Defence Adviser - data sheet only
Scientific Adviser to MRDC, C/- Defence Attache - data sheet only
Head of Staff, British Defence Research and Supply Staff (Australia)
NASA Senior Scientific Representative in Australia
INSPEC: Acquisitions Section Institution of Electrical Engineers
Head Librarian, Australian Nuclear Science and Technology Organisation
Senior Librarian, Hargrave Library, Monash University
Library - Exchange Desk, National Institute of Standards and Technology, US
Exchange Section, British Library Document Supply Centre
Periodicals Recording Section, Science Reference and Information Service, UK
Library, Chemical Abstracts Reference Service
Engineering Societies Library, US
Documents Librarian, The Center for Research Libraries, US

CMDR J.M. Taubman, Deputy Director Submarine Warfare, Canberra